Soil Amplification Factor of Seismic Ground Motions in Laho (PMO), Kumang (SKO) and Sumandak (SBO) in Malaysian Offshore

by

Lee Yik Hoe
13851

Dissertation submitted in partial fulfilment of
the requirements for the
Bachelor of Engineering (Hons)
(Civil)

JANUARY 2015

Universiti Teknologi PETRONAS
Bandar Seri Iskandar
31750 Tronoh
Perak Darul Ridzuan

CERTIFICATION OF APPROVAL

Soil Amplification Factor of Seismic Ground Motions in Laho (PMO), Kumang (SKO) and Sumandak (SBO) in Malaysian Offshore

by

Lee Yik Hoe
13851

A project dissertation submitted to the
Civil Engineering Programme
Universiti Teknologi PETRONAS
in partial fulfilment of the requirements for the
BACHELOR OF ENGINEERING (Hons)
(CIVIL)

Approved by,

_____
(Assoc. Prof. Ir. Dr. Mohd. Shahir Liew)

UNIVERSITI TEKNOLOGI PETRONAS
TRONOH, PEAK
January 2015

CERTIFICATION OF ORIGINALITY

This is to certify that I am responsible for the work submitted in this project, that the original work is my own except as specified in the references and acknowledgements, and that the original work contained herein have not been undertaken or done by unspecified sources or persons.

_____

LEE YIK HOE

ABSTRACT

Distant earthquakes in Sumatra and Sulawesi might possess hazard to the offshore platforms in Malaysia underlain by soft soils as the soils might amplify the seismic waves that reach the bedrock of Malaysia. A study of the soil amplification factors in PMO, SKO and SBO is necessary to reduce the downtime loses and onsite casualties of the offshore platforms. This research is one of the pioneers for Malaysian offshores. Thus, Laho in PMO, Kumang in SKO and Sumandak in SBO are selected as three representative case studies for this research. The shear wave velocities of the soils at the selected sites are estimated using published cone penetration test correlation equation. The input motion is based on the strongest earthquake recorded in MMD station near to the selected sites between year 2004 and 2007. A second analysis is conducted by scaling the earthquake recorded to 0.06g to simulate the shaking caused by an earthquake with a return period of 475 years in Malaysia. One-dimensional equivalent linear site response analysis is selected and performed by DEEPSOIL v5.1. The unscaled earthquakes (PGA= 0.0015g) generate high amplification factors but they are associated with very low levels of earthquake shaking which hardly harm the structure on site. The scaled earthquakes (0.06g) generate relatively lower amplification factors which are caused by the nonlinear behaviour of soils. The scaled earthquake also generates a peak spectral amplification at a longer period. However, the lower amplification factors of 1.6 (period 0.4s-2.0s) and 3.5 (period 3.5s) in Sumandak should be taken into account in the design of structure because they are associated with PGA of 0.06g which is significant enough to damage the platforms on site, especially if the seismic waves are amplified and the structure has a natural period close to the amplified periods. This research also shows that the impedance contrast of shear wave velocities at the boundary of two soil layers amplifies the seismic waves. Besides, the soil amplification factors depend on the intensity of shaking.

ACKNOWLEDGEMENTS

I would like to express my special appreciation and thanks to my supervisor Assoc. Prof. Ir. Dr. Mohd. Shahir Liew. Your guidance throughout the 8-month research project has assisted me in my progress.

I also take this opportunity to express a deep sense of gratitude to Mr. Md. Yazid bin Mansor who is an industry expert in the department of geosciences in UTP for his unselfish sharing of knowledge, experience and constant help.

Furthermore, I would like to thank Universiti Teknologi PETRONAS for providing a platform for research and support throughout the 8 months.

A special thanks to my family. Words cannot express how grateful I am to my mother and father for all of the sacrifices that you've made on my behalf. Your support to me was what sustained me thus far. I would also like to thank all of my friends who accompany me to strive towards my goal. At the end I would like to express my sincere appreciation to Kee Cassy who is always my support in the moments when there is no one to answer my queries.

TABLE OF CONTENTS

LIST OF FIGURES

LIST OF TABLES

ABBREVIATIONS AND NOMENCLATURES

1-D	One-dimensional
CPT	Cone penetration test
MMD	Malaysian Meteorological Department
NEHRP	National Earthquake Hazards Reduction Program
PGA	Peak ground acceleration
PI	Plasticity index
PMO	Peninsular Malaysia Operation
SBO	Sabah Operation
SI	Soil investigation
SKO	Sarawak Operation
SPT	Standard penetration test

LIST OF SYMBOLS

A_{pga}	Amplification of peak ground acceleration
e_o	Void ratio
F_a	Amplification factor (spectral acceleration)
$F_{a,p}$	Peak spectral amplification factor
F_a (0.1-0.5s)	Amplification factor of period ranges from 0.1s to 0.5s
F_a (0.4-2.0s)	Amplification factor of period ranges from 0.4s to 2.0s
f_s	Sleeve friction resistance (CPT)
g	Gravitational acceleration
G	Shear modulus
M_s	Surface-wave magnitude
M_w	Moment magnitude
q_c	Cone tip resistance (CPT)
r^2	Coefficients of determination
S_a	Spectral acceleration
T_s	Fundamental site period
V_s	Shear wave velocity
ξ	Damping ratio
σ'_v	Effective vertical stress

1 INTRODUCTION

1.1 Background

In spite of the strategic location of Peninsular Malaysia and Singapore on the stable part of Eurasian Plate, tremors were felt in buildings underlain by soft soil in these two regions due to distant earthquakes occurred in Sumatra (Balendra, Tan, & Lee, 1990). Lessons learnt from the past suggest that distant earthquake can cause significant damage. In 1985, Mexico City was subjected to an earthquake that has caused 4,000 to lose their lives and 100,000 to lose their homes (Sun & Pan, 1995). The earthquake had a surface wave magnitude (M_s) of 8.1 and the epicentre of the earthquake was located at remarkably 400km away.

Malaysian offshore platforms in Peninsular Malaysia (PMO), Sarawak Operation (SKO) and Sabah Operation (SBO) are set on soft marine soil. The earthquake waves generated in Sumatra have to travel over 600-800 km before reaching the bedrock in PMO. High-frequency earthquake waves are promptly dampened during propagation, whereas long-period waves are more resistant to energy dissipation and consequently they manage to travel long distances (Tan, Majid, Ariffin, & Bunnori, 2014). Therefore, long period or low frequency earthquake waves are able to reach the bedrock of PMO, SKO and SBO. These long period waves might be amplified by site soils depend on their rigidity when they propagate upward (Balendra & Li, 2008). The amplified waves can cause resonate in structures with similar fundamental period to the site soil, causing significant structure vibrations.

1.2 Problem Statement

In February of 1994, Malaysia's neighbour, Singapore had some buildings vibrated due to an earthquake near Liwa, southern Sumatra around 700 km away. The magnitude (M_s) 7.0 earthquake woke up hundreds of people and they ran out of the building in panic (Sun & Pan, 1995). Three months later, in May 1994, an earthquake near Siberut Island, which is 570 km away from Singapore, has set some office buildings in motion. The earthquake was recorded only 6.2 on the Richter scale but has again caused panic to the people that they evacuated from the office buildings (Sun & Pan, 1995). According to Sun and Pan (1995), the buildings in both incidents were underlain by the Quaternary deposits, namely the Kallang Formation. In a like manner, PMO, SKO and SBO Malaysia are located on South China Sea where the site soils might possess similar characteristics and properties as the Kallang Formation. Above all, the Malaysian offshore platforms were not designed for seismic loads!

Moreover, Sun & Pan (1995) found out "that the recurrence interval of an earthquake in Sumatra with a moment magnitude (M_w) of 8.5 or larger is about 340 years, which is equivalent to a 14% probability of exceedance within 50 years" (p. 105). He also added that "the emitted energy of a magnitude 8.5 earthquake is more than 100 times that of the magnitude (M_s) 7.0 Liwa earthquake in 1994" (p. 109).

Due to the fact that Malaysian offshore platforms were not designed for seismic loads and the probability of occurrence of large earthquake in the vicinity of Malaysia is significantly high, it is critical to study the soil amplification factor in the Malaysian offshore to identify the possible hazards on existing platforms and to guide future platform design criteria.

1.3 Objectives

Objective One

Determine the configuration and properties of near surface materials in Laho (PMO), Kumang (SKO) and Sumandak (SBO)

Objective Two

Determine the fundamental site period of Laho (PMO), Kumang (SKO) and Sumandak (SBO)

Objective Three

Determine the soil amplification factors for Laho (PMO), Kumang (SKO) and Sumandak (SBO)

1.4 Scope of Study

The scope of this study covers the one-dimensional site response analysis of Laho (Terengganu offshore, PMO), Kumang (Sarawak offshore, SKO) and Sumandak (Sabah offshore, SBO) based on the information extracted from the soil investigation reports available. Maximum bedrock spectral acceleration in the study area will be obtained and acts as an input in this study. The relationship of ground surface motion and structure responses is not in the scope of this study.

2 LITERATURE REVIEW

2.1 Distant Earthquake Threats

Sun and Pan (1995) pointed out that distant earthquakes in Sumatra might cause damage to structures on soft soil in South East Asia learning from the incident of Mexico City in 1985. In the incident of Mexico City, the epicentre of the earthquake was located near the southern coast of Mexico, around 400 km away. In this region, the Cocos Plate subducts under the North America plate at a rate of about 55mm per year (DeMets, Gordon, Argus, & Stein, 1990). The earthquake had a surface wave magnitude (M_s) of 8.1 and caused at least 4000 people to lose their lives and 100,000 were left homeless (Sun & Pan, 1995). The unexpectedly serious damages were concentrated in an area underlain by soft soils (Booth, Pappin, Mills, Degg, & Steedman, 1986). Mexico City is built partially on soft Quaternary deposits. The peak ground acceleration recorded on hard rock was less than 3-4% of the gravity acceleration, but that recorded on soft soil was more than 20% of the gravity acceleration (Booth et al., 1986). It is obvious that the earthquake waves were amplified locally by the surface layer of soft soils.

2.2 Earthquake in vicinity of Malaysia

From the findings of Sun and Pan (1995), the magnitude of an earthquake in Sumatra with a probability of exceedance of 10% in 50 years is found to be 8.56. They (Sun & Pan, 1995) highlighted that this figure is too high to be ignored in Malaysia and the energy emitted during an 8.5 earthquake is more than 100 times of that magnitude (M_s) 7.0 Liwa Earthquake and more than 2000 times of that magnitude 6.2 Siberut earthquake in which both the earthquakes have caused tremors to be felt in Singapore.

2.3 Tremors Felt in Malaysia and Singapore

Some buildings in Singapore experienced tremors due to earthquake of magnitude (M_s) 7.0 near Liwa in southern Sumatra more than 700km away and earthquake near Siberut Island, 570 km away, which measure only 6.2 on the Richter scale (Sun & Pan, 1995). In both incidents, the buildings are located in the south-eastern part of Singapore Island, underlain by the Quaternary deposits, namely the Kallang

Formation. Sun and Pan (1995) also mentioned that the Siberut Island earthquake caused tremors in Kuala Lumpur.

2.4 Attenuation Model

On the other hand, Balendra and Li (2008) successfully found out that Component Attenuation Model (CAM) predicts the bedrock motion in Singapore caused by earthquakes in the subduction region of the Indonesian Arc and Burmese Arc reliably and accurately for prediction up to 600km. Based on the verified CAM model, Balendra and Li (2008) proceed to generate synthetic bedrock accelerograms and thus maximum bedrock spectral acceleration for M_w= 9.5 and M_w= 7.8 earthquake using a stochastic simulation program named GENQKE (Lam & Wilson, 1999). The predominant period of the bedrock motions, the period of the site and the period of the building must coincide for the worst situations. From the data generated by GENQKE, sites with periods between 1.6s and 1.85s would respond severely to the bedrock motions due to the M_w= 9.5 earthquake in Sumatran subduction fault, and that sites with a period of 0.7s would resonate to the bedrock motions due to the M_w=7.8 earthquake in Sumatran fault. The sites with natural periods of 0.7s to 1.85s would be of interest.

2.5 Mechanism of Soil Amplification

Sun and Pan (1995) explained the phenomena in a simplified way as resonance. The shear wave velocities are very different between the surface material and the bedrock. The shear wave velocities of surface material can be below 100 m s^{-1} while bedrock is normally above 2000 m s^{-1}. The difference makes the boundary between soft and hard layers a surface of reflection, “trapping” the numerous cycles of incoming waves and when the waves are in phase of each other, a much stronger wave is produced. Thickness of each soil layer, its shear wave velocity and the fundamental site period of the subsurface condition are the primary parameters that affect seismic soil amplification in particular sites (Tan et al., 2014).

On the other hand, Street, Woolery, Wang, and Harris (2001) have a similar understanding that the properties and configuration of soils highly affect the amplitude, frequency and duration characteristics of seismic waves that propagate through them. The critical property is the impedance contrasts at the boundaries

between media of differing velocities and densities. Besides, stiffness and damping of the materials that make up the layers are important. Shear waves from an earthquake are commonly assumed to propagate vertically upward from the underlying bedrock because of the sharp impedance contrast between the bedrock and overlying soils.

2.6 Shear Wave Velocities

Booth et al. (1986) reported that the area of high damage in Mexico City occurred over a 40m thick soft layer of lacustrine deposit with water content of 200-400% whose shear wave velocity is about 80 m s^{-1}, and the amplified wave has a dominant frequency of 0.5 Hz. Therefore, buildings with a natural period of 2 s experienced resonant amplification and disaster happened.

Shear wave velocities of the soil are required for the calculation of natural site period and thus its amplification factor. Empirical formulas which relate Standard Penetration Test (SPT) values to shear wave velocity are developed by researchers all around the world. A summary of established correlation in half of the past century is listed in the table below (Marto, Soon, Kasim, & Suhatril, 2013).

Researcher	All soil	Cohesionless soil	Cohesive soil
Kanai (1966)	$Vs = 19N^{0.6}$		
Ohba and Toriumi (1970)	$Vs = 84N^{0.31}$		
Shibata (1970)		$Vs = 32N^{0.5}$	
Imai and Yahimura (1970)	$Vs = 76N^{0.33}$		
Ohta *et al.* (1972)		$Vs = 87N^{0.36}$	
Fujimara (1972)	$Vs = 92.1N^{0.337}$		
Ohsaki and Iwasaki (1973)	$Vs = 81.4N^{0.39}$	$Vs = 59.4N^{0.47}$	
Imai and Yoshimura (1975)	$Vs = 92N^{0.329}$		
Imai *et al.* (1975)	$Vs = 89.9N^{0.341}$		
Imai (1977)	$Vs = 91N^{0.337}$	$Vs = 80.6N^{0.331}$	$Vs = 102N^{0.292}$
Ohta and Goto (1978)	$Vs = 85.35N^{0.348}$	$Vs = 88N^{0.34}$	
JRA (1980)		$Vs = 80N^{0.33}$	$Vs = 100N^{0.33}$
Seed and Idriss (1981)	$Vs = 61.4N^{0.5}$		
Imai and Tonouchi (1982)	$Vs = 97N^{0.314}$		
Seed *et al.* (1983)		$Vs = 56.4N^{0.5}$	
Sykora and Stokoe (1983)		$Vs = 100.5N^{0.29}$	
Okamoto *et al.* (1989)		$Vs = 125N^{0.3}$	
Lee (1990)		$Vs = 57.4N^{0.49}$	$Vs = 114.43N^{0.31}$
Imai and Yoshimura (1990)	$Vs = 76N^{0.33}$		
Yokota *et al.* (1991)	$Vs = 121N^{0.27}$		
Kalteziotis *et al.* (1992)	$Vs = 76.2N^{0.24}$	$Vs = 49.1N^{0.49}$	$Vs = 76.6N^{0.45}$
Raptakis *et al.* (1995)		$Vs = 100N^{0.24}$	$Vs = 184.2N^{0.17}$
Athanasopoulos (1995)	$Vs = 107.6N^{0.36}$		
Sisman (1995)	$Vs = 32.8N^{0.51}$		
Iyisan (1996)	$Vs = 51.5N^{0.316}$		
Jafari *et al.* (1997)	$Vs = 22N^{0.85}$		
Chien *et al.* (2000)		$Vs = 22N^{0.75}$	
Kiku *et al.* (2001)	$Vs = 68.3N^{0.292}$		
Jafari *et al.* (2002)	$Vs = 22N^{0.85}$	$Vs = 19N^{0.85}$	$Vs = 27N^{0.73}$
Hasancebi and Ulusay (2007)	$Vs = 90N^{0.309}$	$Vs = 90.82N^{0.319}$	$Vs = 97.89N^{0.269}$
Hanumantharao and Ramana (2008)	$Vs = 82.6N^{0.43}$	$Vs = 79N^{0.434}$	
Lee and Tsai (2008)	$Vs = 137.153N^{0.229}$	$Vs = 98.07N^{0.305}$	$Vs = 163.15N^{0.232}$
Dikmen (2009)	$Vs = 58N^{0.39}$	$Vs = 73N^{0.33}$	$Vs = 44N^{0.48}$
Brandenberg *et al.* (2010)			
Uma Maheswari *et al.* (2010)	$Vs = 95.64N^{0.301}$	$Vs = 100.53N^{0.293}$	$Vs = 89.31N^{0.356}$
Tsiambaos and Sabatakakis (2011)	$Vs = 105.7N^{0.327}$	$Vs = 79.7N^{0.301}$	$Vs = 88.8N^{0.378}$
Anbazhagan *et al.* (2012)	$Vs = 68.96N^{0.51}$	$Vs = 60.17N^{0.58}$	$Vs = 106.63N^{0.39}$

A: controls the amplitude
B: controls the relationship curvature

Figure 1 List of standard penetration test correlation equation to shear wave velocities

On the other hand, Wair, DeJong, and Shantz (2012) has summarised a list of cone penetration test (CPT) correlation equation to shear wave velocities (V_s). In addition to penetration resistance, the incorporation of geologic age, confining stress and soil type can further increase the prediction accuracy. There are two types of published CPT-V_s correlation equations presented in Figure 2. The first type of equation was developed for specific soil types (sand/ clay) whereas the second type of equation was developed for more general all soils. In the study done by Wair et al. (2012), two methods were used to estimate the shear wave velocities. The first method used the equation developed for all soil type and the second method used the equation developed for specific soil types. It was found out that both type of equation performed similarly according to their statistic. On average, the soil type-specific equation under-predicted the shear wave velocities by approximately 8% and the all soils equation under-predicted the shear wave velocities by approximately 3% (Wair et al., 2012). The soil type-specific method produced spikes (high and low) in the predicted V_s profile at material transitions where difference equations were used for adjacent CPT sub-layers. For this reason, as well as, ease of implementation, the all soils method was considered to be more desirable.

Soil Type	Study	Geologic Age	Number of Data Pairs	r^2	V_S (m/s)	(Eq #)
All Soils	Hegazy & Mayne (1995)	Quaternary	323	0.70	$(10.1 \log(q_c) - 11.4)^{1.67} (100\, f_s/q_c)^{0.3}$	(5.6)
	Mayne (2006)	Quaternary	161	0.82	$118.8 \log(f_s) + 18.5$	(5.7)
	Piratheepan (2002)	Holocene	60	0.73	$32.3\, q_c^{0.088}\, f_s^{0.121}\, D^{0.235}$	(5.8)
	Andrus et al. (2007)	Holocene & Pleistocene	185	(H) 0.71 (P) 0.43	$2.62\, q_t^{0.395}\, I_C^{0.912}\, D^{0.124}\, SF^a$	(5.9)
	Robertson (2009)	Quaternary	1,035	—	$[(10^{(0.55 I_C + 1.68)})\, (q_t - \sigma_{vo}) / p_a]^{0.5}$	(5.10)
Sand	Sykora & Stokoe (1983)	—	256	0.61	$134.1 + 0.0052\, q_c$	(5.11)
	Baldi et al. (1989)	Holocene	—	—	$17.48\, q_c^{0.13}\, \sigma'^{0.27}_v$	(5.12)
	Hegazy & Mayne (1995)	Quaternary	133	0.68	$13.18\, q_c^{0.192}\, \sigma'^{0.179}_v$	(5.13)
	Hegazy & Mayne (1995)	Quaternary	92	0.57	$12.02\, q_c^{0.219}\, f_s^{-0.0466}$	(5.14)
	Piratheepan (2002)	Holocene	25	0.74	$25.3\, q_c^{0.183}\, f_s^{0.029}\, D^{0.155}$	(5.15)
Clay	Hegazy & Mayne (1995)	Quaternary	406	0.89	$14.13\, q_c^{0.339}\, e_0^{-0.473}$	(5.16)
	Hegazy & Mayne (1995)	Quaternary	229	0.78	$3.18\, q_c^{0.548}\, f_s^{0.025}$	(5.17)
	Mayne & Rix (1995)	Quaternary	339	0.83	$9.44\, q_c^{0.435} e_0^{-0.522}$	(5.18)
	Mayne & Rix (1995)	Quaternary	481	0.74	$1.75\, q_c^{0.627}$	(5.19)
	Piratheepan (2002)	Holocene	20	0.91	$11.9\, q_c^{0.269}\, f_s^{0.108}\, D^{0.127}$	(5.20)

Units: q_c, q_t, f_s, σ_{vo}, and σ'_{vo} are measured in kilopascals (kPa), and depth (D) is measured in meters (m). p_a = 100 kPa.
[a]SF = 0.92 for Holocene and 1.12 for Pleistocene

Figure 2 List of cone penetration test correlation equation to shear wave velocities

National Earthquake Hazards Reduction Program (NEHRP) site classification takes into account the shear wave velocity of the upper 30m of sediments and/or rocks (BSSC, 2003). NEHRP categorises soils into class A, B, C, D, E or F based on their vertical shear-wave profile, thickness and liquefaction potential. The NEHRP shear wave velocity (V_S) assigned to the subsurface at a specific site is calculated using the following formula:

$$\overline{V_S} = \frac{\sum_{i=1}^{n} d_i}{\sum_{i=1}^{n} \frac{d_i}{v_S}}$$

where:

$\overline{V_S}$ = the N she w v

v_S = the she w v o a l in m/s

d_i = the thic o a l (b 0 a 30 m)

The table below is prepared by NEHRP. It shows the site classification system according to the shear wave velocity of the upper 30m sediments or rocks.

Table 1 National Earthquake Hazards Reduction Program (NEHRP) site classification system

Soil type NEHRP	General description	Average shear wave velocity to 30 m (m/s)
A	Hard rock	> 1500
B	Rock	$760 < V_S \leq 1500$
C	Very dense soil and soft rock	$360 < V_S \leq 720$
D	Stiff soil $15 \leq N \leq 50$ or $50\ kPa \leq Su \leq 100\ kPa$	$180 < V_S \leq 360$
E	Soil or any profile with more than 3 m of soft clay defiled as soil with PI > 20, w ≥ 40%, and Su < 25 kPa	≤ 180
F	Soils requiring site-specific evaluations	

D'Appolonia (2009) has modified the NEHRP table so that it suits the geologic condition of Malaysia. Table 2 shows the modified table that classifies the site class according to the average properties in top 30m of effective seabed.

Table 2 Modified Malaysian Site Class by D'Appolonia

SITE CLASS	SOIL PROFILE NAME	AVERAGE PROPERTIES IN TOP 30m OF EFFECTIVE SEABED		
		Soil shear wave velocity Vs,30 (m/s)	Sand: normalized cone penetration resistance qcl,30(1) (bar)	Clay: soil undrained shear strength Cu,30 (kPa)
A	Hard rock	> 1500	Not Applicable	Not Applicable
B	Rock, thickness of soft sediments < 5 m	750 - 1500	Not Applicable	Not Applicable
C	Very dense hard soil and soft rock	350 - 750	> 200	> 200
D	Stiff to very stiff soil	180 - 350	80 - 200	80 - 200
E	Soft to firm soil	120 - 180	< 80	< 80
F1	Very soft NC clay	80 - 120	Minimum sand component	Consistent with Vs
F2	-	Any profile, including those otherwise classified as A to F1, containing soils having one or more of the following characteristics: • Vs,30 < 80 m/s • Soils vulnerable to potential failure or collapse under seismic actions such as liquefiable soils, highly sensitive clays, collapsible weakly cemented soils; • Ooze (clay containing more than 30% calcareous or siliceous material of biogenic origin) with a thickness of more than 10 m; • Soil layers with high gas content or ambient excess pore pressure greater than 30 % of in situ effective overburden • Layers greater than 2 m thick with sharp contrast in shear wave velocity (greater than ± 30 %) and/or undrained shear strength (greater than ± 50 %) compared to adjacent layers		

However, Street et al. (2001) pointed out the possible shortcomings of the NEHRP soil classification are that the effects of the deeper (>30 m) sediments and the large impedance contrast at the bedrock/sediment interface are not necessarily accounted for by this methodology.

2.7 One-Dimensional (1-D) Site Response Analysis

1-D site response analysis assume that waves propagate in one direction only and the motion is identical on planes perpendicular to that motion. This method cannot handle refraction so the layer boundaries must be perpendicular to the direction of wave propagation and the usual assumption is vertically-propagating shear (SH) waves.

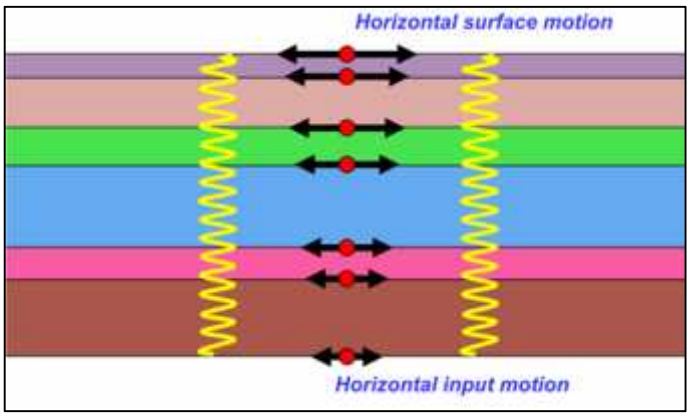

Figure 3 Vertically-propagating shear waves causing horizontal surface motion

In 1-D site response analysis, the input (object) motion can be modeled in two different ways depending on where the motion is recorded. If an outcrop motion is being used, bedrock should be modelled as an elastic half-space. If a within motion is being used, bedrock should be modelled as a rigid half-space (Hashash, Groholski, Phillips, Park, & Musgrove, 2012).

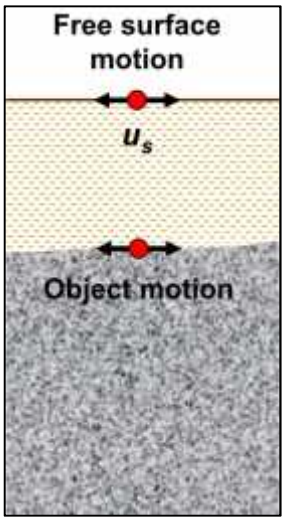

Figure 4 Diagram of input motion and free surface motion

The first method of 1-D site response analysis is complex response method. It is the approach used in computer programs like SHAKE2000 (Deng & Ostadan, 2000). Transfer function is used with input motion to compute surface motion. For layered profiles, transfer function is "built" layer by layer to go from input motion to surface motion. Complex response method is a linear analysis and it operates in frequency domain. Input motion represented as sum of series of sine waves. Then, the solution for each sine wave is obtained and added together to get the total response.

Nevertheless, soils exhibit nonlinear, inelastic behaviour under cyclic loading conditions. Their stiffness decreases and damping increases as cyclic strain amplitude increases. The nonlinear, inelastic stress-strain behaviour of cyclically loaded soils can be approximated by equivalent linear properties. (Hashash et al., 2012)

<u>Steps of 1-D Equivalent Linear Site Response Analysis</u>

1. Assume some initial strain and use to estimate G and ξ using the shear modulus curve and damping curve.
2. Use these values to compute response.

3. Determine peak strain and effective strain.
4. Select new G and ξ from the shear modulus curve and damping curve based on updated strain level.
5. Compute response with new properties and determine resulting effective shear strain
6. Repeat until computed effective strains are consistent with assumed effective strains.

   (Hashash et al., 2012)

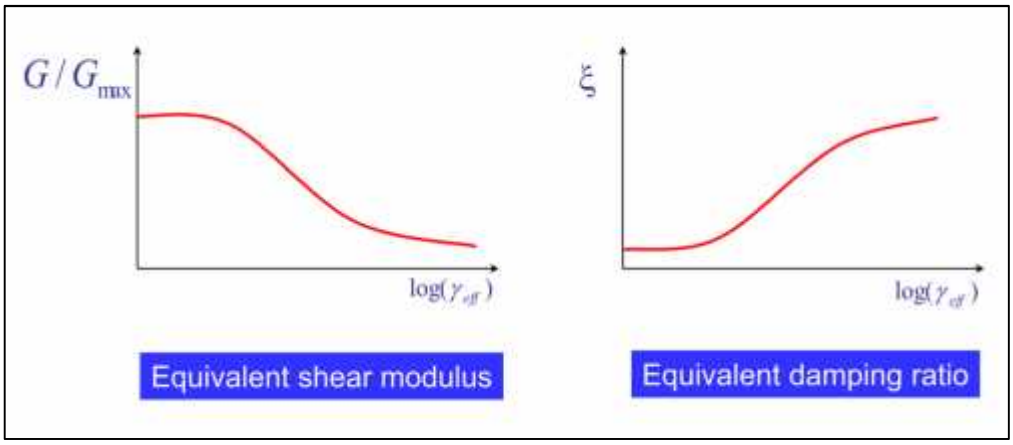

Figure 5 Modulus reduction curve and damping curve for equivalent linear site response analysis

The advantages of equivalent linear approach are:

i. Can work in frequency domain
   - Compute transfer function at relatively small number of frequencies as compared to calculating each time interval in time series

ii. Equivalent linear properties readily available for many soils

iii. Can make first-order approximation to effects of nonlinearity and inelasticity within framework of a linear model.

2.8 Related Studies

Balendra and Li (2008) inputted the borehole data of 3 selected sites in the Quaternary deposits in Singapore and their bedrock accelerograms generated by GENQKE (Lam & Wilson, 1999) into the computer program SHAKE91 to calculate the resultant surface motions, acceleration response spectra at surface and amplification factors. The results found were the maximum spectral acceleration of the M_w= 9.5 earthquake is 95.8 gals for the site with period of 1.6s to 1.8s, and that

of the M_w=7.8 earthquake is 98.9 gals for the site period of 0.7s (Balendra & Li, 2008). The maximum elastic base shear that would be induced in a building with a period in the range 0.7 to 1.8 sec due to the worst earthquake scenario is nearly 10% of the weight of the building (Balendra & Li, 2008).

Furthermore, Mahajan (2009) conducted a study of Dehradun fan deposits in India, found out that attenuation is greater on the south-western side of the Dehradun fan deposits (thicker, low velocity sediments) which the sites had been classified as class 'D' and 'E' but the site amplification tends to be greater in the northern and north-western part of the city due to large impedance contrast within the near surface soils.

3 METHODOLOGY

The methodology is designed as a step by step approach to achieve the stated objectives. There are several project activities in this research and each project activity will be described in structure and detail in the following order.

3.1 Extraction of Information from Soil Investigation (SI) Report of Selected Sites

First of all, the SI reports of Laho (PMO), Kumang (SKO) and Sumandak (SBO) are obtained. It should be noted that the field tests of SI were carried out by cone penetrometer with pore pressure measurements (CPTU). The exact coordinates of the borehole location in which the SI was carried out are listed in the table below.

Table 3 Coordinates of borehole location of soil investigation reports

Operation	Location	Borehole Location	Actual Position		Geotechnical Investigation Report No. *(for reference)*
			Latitude	Longitude	
PMO	Laho	BH-LA	6° 19' 40.485"	104° 02' 09.953"	KUA/03-03/0014A(III)
SKO	Kumang	BH KAJT-A	*Easting (m) 607,219.34*	*Northing (m) 487,787.85*	BTU/02-07/0261
SBO	Sumandak-A	BH-1AR	5° 37' 17.044"	114° 59' 31.378"	LBU/05-04/0039

Secondly, all the relevant information required for this research is extracted from the SI reports. The information includes:

i. Soil layers and their description
ii. Thickness of each soil layer
iii. Unit weight of soil
iv. Sleeve friction resistance, f_s (CPT)
v. Corrected cone resistance, q_t (CPT)
vi. Porosity of soil
vii. Plasticity Index (PI) of Soil

3.2 Determination of Shear Wave Velocities, V_s of Each Soil Layer Using Cone Penetration Test (CPT) Correlation Equations

The geologic age of soils in PMO, SKO and SBO are Quaternary and hence CPT-V_s correlation equations which were developed for Quaternary soils are chosen. (Wair et al. (2012)) have summarised the V_s prediction equations developed for Quaternary soils from various sites worldwide. Each correlation equation was developed with different number of data pairs and has different coefficients of determination (r^2). The closer the coefficients of determination (r^2) to 1, the greater the agreement between the V_s estimated and V_s measured.

The correlation equations are chosen after considering the number of data pairs and coefficients of determination. In other words, all the correlation equations chosen for this research are reliable as they have large number of data pairs and high coefficients of determination.

The following section will state the correlation equations chosen for each site and their description.

Laho and Kumang

The CPT-V_s correlation equation chosen for clay and sand is

$V_s = 118.8 \log(f_s) + 18.5$ *for all Quaternary soils* (Mayne, 2006)

This equation is chosen because it has a high coefficient of determination of 0.823. Additionally, the correlation between V_s and f_s (CPT) of this equation is based on regression of a large dataset (161 data pairs) from numerous sites around the world. This method is in accordance to the first method proposed by Wair et al. (2012) to use the all soils equation as explained in chapter 2.6. The advantage of this method is to avoid spikes (high and low) in the predicted V_s profile at material transitions where difference equations were used for adjacent CPT sub-layers.

Sumandak

The CPT-V_s correlation equation chosen for clay are

$V_s = 14.13\, q_c^{0.3}\, e_c^{-0.4}$ *for clay* (Hegazy & Mayne, 1995)

$V_S = 3.18\, q_c^{0.5}\ \ f_s^{0.0}$ *for clay* (Hegazy & Mayne, 1995)

$V_S = 9.44\, q_c^{0.4}\ \ e_c^{-0.5}$ *for clay* (Mayne & Rix, 1995)

$V_S = 1.75\, q_c^{0.6}$ *for clay* (Mayne & Rix, 1995)

The CPT-V_s correlation equation chosen for sand are

$V_S = (10.1 \log(q_c) - 11.4)^{1.6}\ (100^{f_s/q_c})^{0.3}$

for all Quaternary soils (Hegazy & Mayne, 1995)

$V_S = 118.8\ \log(f_s) + 18.5$ *for all Quaternary soils* (Mayne, 2006)

$V_S = 134.1 + 0.0052 q_c$ *for sand* (Sykora & Stokoe, 1983)

$V_S = 13.18\, q_c^{0.1}\ \ \sigma_v'^{0.1}$ *for sand* (Hegazy & Mayne, 1995)

The shear wave velocities predicted for clay are the average of the estimated values from the clay CPT-V_s correlation equations. Similarly, the shear wave velocities predicted for sand are the average of the estimated values from the sand CPT-V_s correlation equations. This method is in accordance to the second method proposed by Wair et al. (2012) to use the soil type-specific equation. It should be emphasised that both methods (first method is used for Laho and Kumang and second method is used for Sumandak) have been statistically proven to perform similarly (Wair et al., 2012).

All the prediction equations chosen above for site Sumandak have a high coefficient of determination (r^2). The coefficients of determination (r^2) range from 0.61 to 0.89. Furthermore, they have a huge number of data pairs ranging from 161 to 481 data pairs.

The reason that only one V_s prediction equation is used for Laho and Kumang while average value of several V_s prediction equations is used for site Sumandak is to allow future comparison of site measured V_s with the estimated V_s. The comparison result will provide an insight to which whether V_s prediction equation for all soils or V_s prediction equation for a particular soil type is more suitable to be applied in the Malaysian offshore soils.

The second reason is to take into account the possible limitation of applying only one equation for one site. The only equation might give an accurate value for a lower bound estimation and an inaccurate value for a higher bound estimation. Therefore, by having two methods in this research, it allows for future comparison with measured data once it is made available.

3.3 Determination of Fundamental Site Period

Calculate the fundamental site period using the formula below

$$T_S = 4 \sum \frac{H_i}{V_S}$$

where H_i = thickness of ith soil layer

V_{si} = V_s of ith layer (Kramer, 1996)

3.4 Determine the Strongest Felt Earthquake Recorded in MMD Station Near to the Selected Sites

The location of the three selected sites in Malaysian offshore are shown in the map below:

Figure 6 Location of Laho, Kumang and Sumandak in Malaysian offshore

The nearest Malaysian Meteorological Department (MMD) seismic stations to the three selected sites are identified so that the earthquake time series recorded at those station can be used as an input for this research.

The nearest MMD seismic station to Laho is Kuala Terengganu weak motion station. On the other hand, the nearest MMD seismic station to Kumang is Bintulu and Sibu weak motion station. Lastly, the nearest MMD seismic station to Sumandak is Sepulut weak motion station and Ranau strong motion station.

The time series of felt earthquake available for this research are from year 2004 to year 2007 only. Each time series of felt earthquake was gone through to identify the one that give the highest peak ground acceleration (PGA) in the MMD seismic station nearest to the three selected sites. The earthquakes that caused highest PGA recorded for each selected site are listed below.

Table 4 Earthquakes that caused the highest peak ground acceleration recorded at the MMD station nearest to the selected sites

	Station	Year	East (g)	North (g)	Vertical (g)
Laho	Terengganu- KTM	SUMATERA EQ 280305 1609UTC	-0.000978	0.001283	0.001301
Kumang	Bintulu- BTM	BINTULU EQ 010504 2329UTC	0.001715	-0.001476	-0.000774
Sumandak-A	Bintulu- BTM	BINTULU EQ 010504 2329UTC	0.001715	-0.001476	-0.000774

It should be noted that there is no significant earthquake recorded at the MMD stations near to Sumandak. Therefore, the time series of Bintulu earthquake recorded at Bintulu weak motion station will be used as an input for the analysis of site Sumandak.

A second analysis is performed for each selected site after the PGA of the input time series is scaled to 0.06g which is correspondent to PGA of earthquake with a return period of 475 years in PMO, SKO and SBO. The recorded PGA is relatively small and therefore the second analysis is designed to simulate a significant earthquake that might happen.

3.5 Input Required Data into DEEPSOIL

As explained in chapter 2.7, DEEPSOIL v5.1 is a one-dimensional site response analysis program. The method chosen for this research is equivalent linear approach because of the reasons stated in chapter 2.7.

Information is inputted into program DEEPSOIL v5.1 in a step by step manner

1. Select “Equivalent Linear Frequency Domain” as the analysis method.
2. Key in the number of soil layers and the depth of water table.

3. For each soil layer the following data is inputted:
    a) Layer name
    b) Thickness
    c) Unit weight
    d) Shear wave velocity
4. Select modulus reduction curve and damping curve for each soil layer
    - For clay, the curves of Vucetic & Dobry, 1991 are selected and the plasticity index is inputted.
    - For sand, the curves of Seed & Idriss, 1991 (mean limit) are selected.
5. Select the option "Elastic Half-Space" and input the bedrock properties as follow:
    - Shear velocity : 1000 m/s
    - Unit weight : 20 kN/m^3
    - Dampition Ratio : 2 %
6. Select the input motion file (time series) and select the layers to generate time history output.
7. Run the analysis.
8. Output is generated which includes:
    a) Acceleration (g) vs Time (s)
    b) Response Spectra: Peak Spectral Acceleration (g) vs Period (s)
    c) Peak Ground Acceleration (g) Profile

3.6 Organise Output Data for Analysis and Interpretation

The output time series and response spectra are organised into a same graph for comparison. The soil amplification factors are determined and certain trends in the graphs are identified. The result are discussed, analysed and interpreted in the following section.

4 RESULTS AND DISCUSSION

4.1 Sumandak

4.1.1 Soil Profile

Table 5 Sumandak: Soil layers and their properties

Layer	Layer Name	Thickness (m)	Unit Weight (kN/m^3)	Average Shear Velocity (m/s)
1	Very soft to soft CLAY	17	15.81	60.28
2	Stiff CLAY	4	18.81	207.41
3	Very Stiff CLAY	4	18.81	299.52
4	Very Stiff CLAY	9.5	18.81	193.46
5	Hard CLAY	5.2	18.81	288.62
6	Very Stiff CLAY	2.8	18.81	233.82
7	Hard CLAY	6.3	18.81	297.69
8	Very Stiff CLAY	4.7	18.81	270.64
9	Very Stiff CLAY	2.8	18.81	264.26
10	Very stiff CLAY	12.7	18.81	276.36
11	Medium dense SAND	15	18.81	207.47
12	Medium dense SAND	7	18.81	208.73
13	Medium dense SAND	5.8	18.81	209.41
14	Hard CLAY	8.2	18.81	362.83
15	Medium dense SAND	9	18.81	210.89
16	Hard CLAY	11	18.81	365.02
17	Very dense SAND	7.7	18.81	245.11
18	Medium dense SAND	12.3	18.81	213.25
19	Hard CLAY	4	18.81	386.21
20	Dense SAND	1	18.81	228.21

Fundamental site period

$$T_S = 4 \sum \frac{H_i}{V_S} = 4 \times 0.82161 = 3.29s$$

where H_i = thickness of ith soil layer

V_{si} = V_s of ith layer (Kramer, 1996)

4.1.2 Seismic Ground Response based on Bintulu Earthquake on 1 May 2004

Ground Acceleration Time History

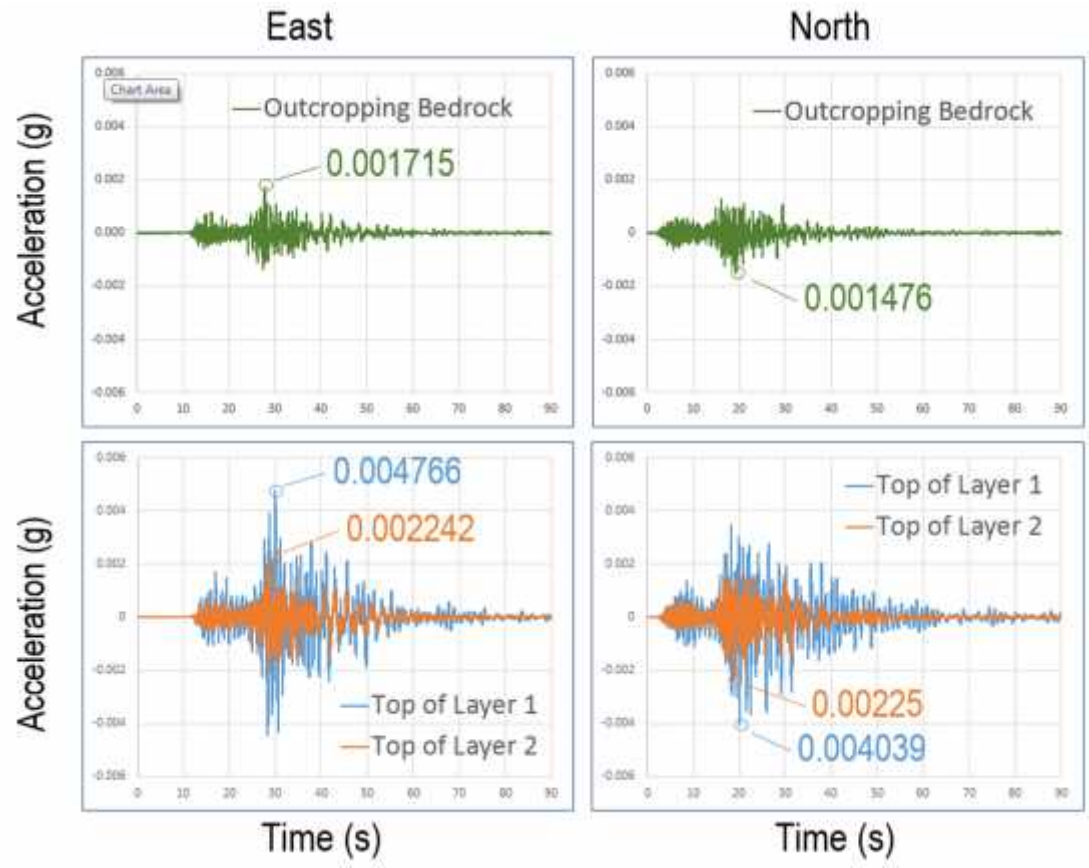

Figure 7 Sumandak: Time series of bedrock motion and soil layers due to Bintulu Earthquake on 1 May 2004

Amplification of Peak Ground Acceleration (A_{pga})

Table 6 Sumandak: Amplification of peak ground acceleration (A_{pga}) due to Bintulu earthquake on 1 May 2004

	East	North
Layer 1	2.78	2.74
Layer 2	1.31	1.52

The amplification of PGA at the top of layer 1 in the east and north direction are 2.78 and 2.74 respectively whereas for the top of layer 2 in the east and north direction are 1.31 and 1.52 respectively. It should be noted that layer 1 comprises of very soft clay with thickness of 17 m and it has a shear wave velocity of 60.28 m/s. On the other hand, the soils extending from the top of the layer 2 to the end of borehole at depth of 150 m are having a shear wave velocities of more than 200 m/s. It is the impedance contrast of shear wave velocities at the boundary of layer 1 and layer 2 that amplifies

the seismic waves. Thus, causing a greater PGA on top of layer 1 as compared to the top of layer 2. Figure 8 and figure 9 below shows the maximum PGA vs. depth for the east direction and north direction.

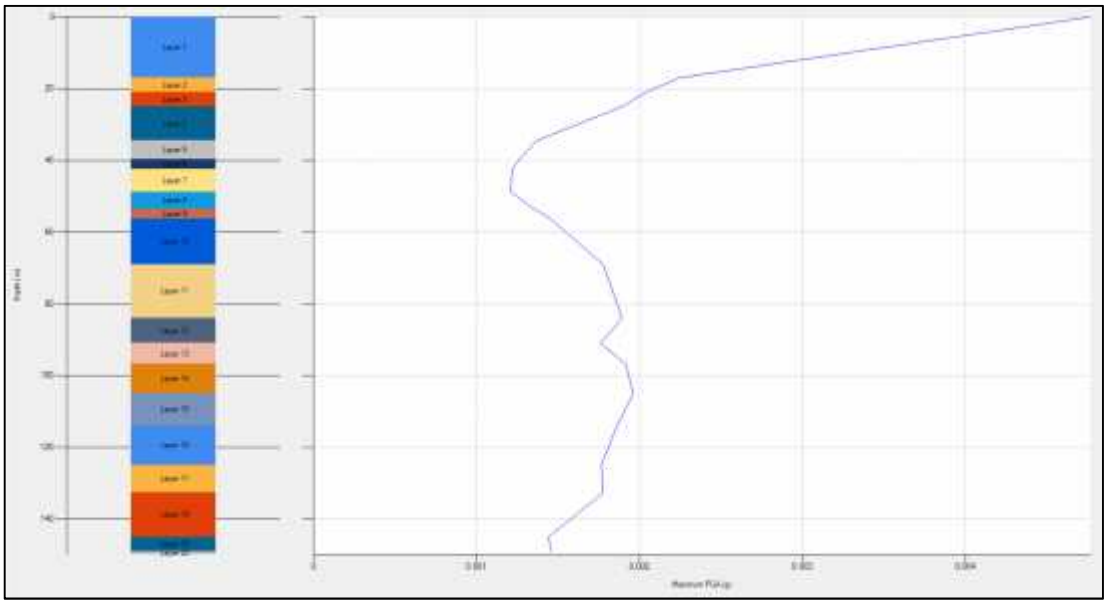

Figure 8 Sumandak: Graph of maximum peak ground acceleration vs. depth in the east direction

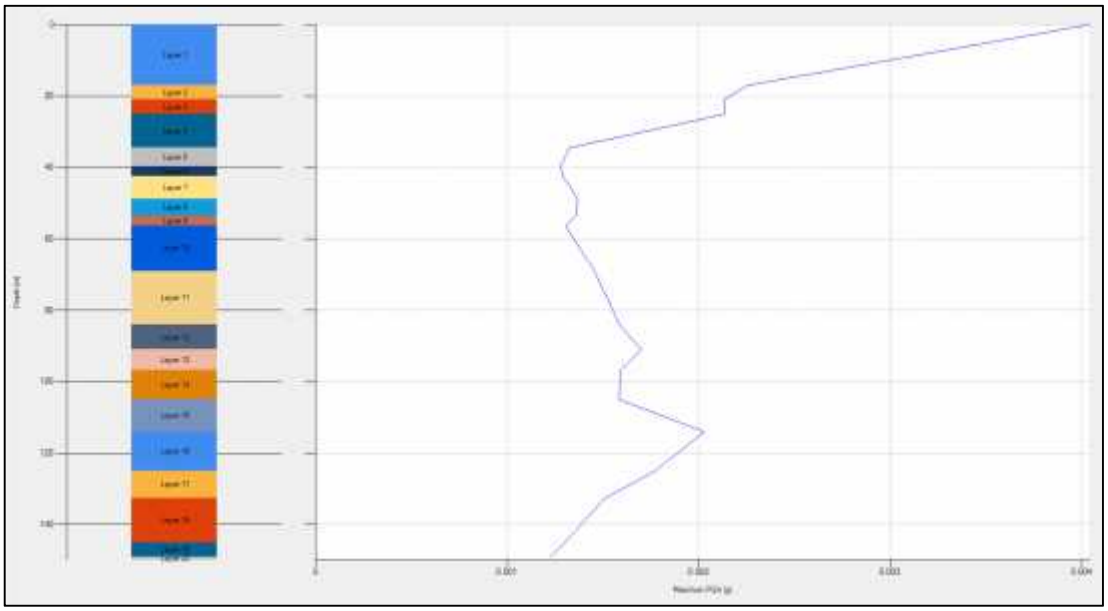

Figure 9 Sumandak: Graph of maximum peak ground acceleration vs. depth in the north direction

Fourier Spectra, Response Spectra and Amplification of Response Spectra (F_a)

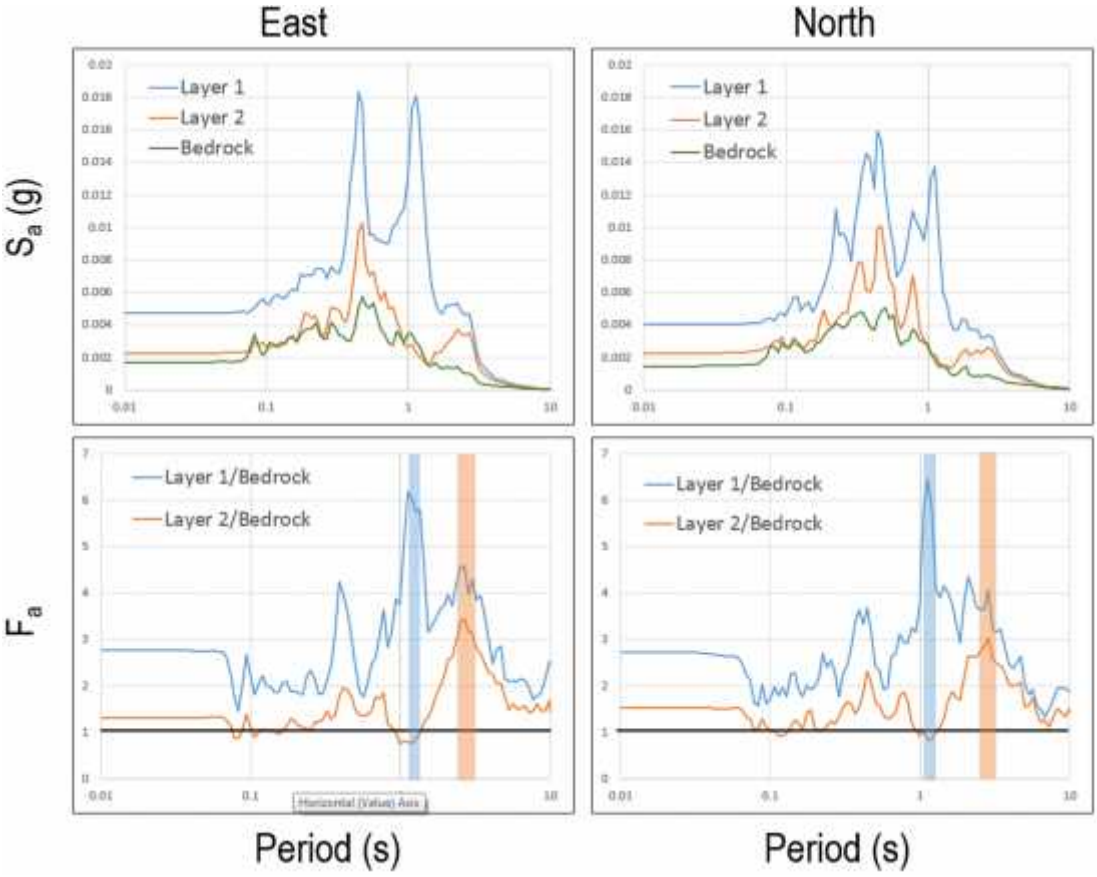

Figure 10 Sumandak: Fourier spectra, response spectra and amplification of response spectra (F_a) due to Bintulu Earthquake on 1 May 2004

It can be seen from the graph of amplification of response spectra that layer 1 is amplified for the whole range of period in both direction. Similarly, layer 2 is amplified for almost the whole range of period. In the east direction, the peak spectral amplification for layer 1 is 6.174 which happens at period 1.125s and for layer 2 is 3.443 at period 2.6858s. In the north direction, the peak spectral 'amplification' for layer 1 is 6.446 which happens at period 1.125s and for layer 2 is 3.041 at period 2.858s. It is observed that the soft soil in layer 1 tends to amplify the incoming seismic waves at period closer to 1.1s whereas the stiffer soil in layer 2 tends to amplify the seismic waves of period 2.7s.

Table 7 Sumandak: Peak spectral amplification ($F_{a,p}$) and amplification factor (F_a) at 0.0015g earthquake

Layer	F_a	East	North
Layer 1/ Bedrock	$F_{a,p}$	6.17 @ 1.125s	6.45 @ 1.125s
	F_a (0.1-0.5s)	2.34	2.38
	F_a (0.4-2.0s)	3.66	3.55
Layer 2/ Bedrock	$F_{a,p}$	3.44 @ 2.6858s	3.04 @ 2.858s
	F_a (0.1-0.5s)	1.26	1.34
	F_a (0.4-2.0s)	1.44	1.54

The amplification factors, F_a (0.1-0.5s) and F_a (0.4-2.0s) are obtained as the average ratios of Fourier spectra over two period ranges, 0.1 to 0.5s and 0.4 to 2.0s. The period ranges correspond to those used for obtaining average amplification factors for the NEHRP Provisions (BSSC, 2003). The amplification factors are shown in the table above. The peak acceleration at the surface is only about 0.0015g, so the amplification factors are associated with very low levels of earthquake shaking.

4.1.3 Seismic Ground Response based on Bintulu Earthquake on 1 May 2004 scaled to 0.06g

Ground Acceleration Time History

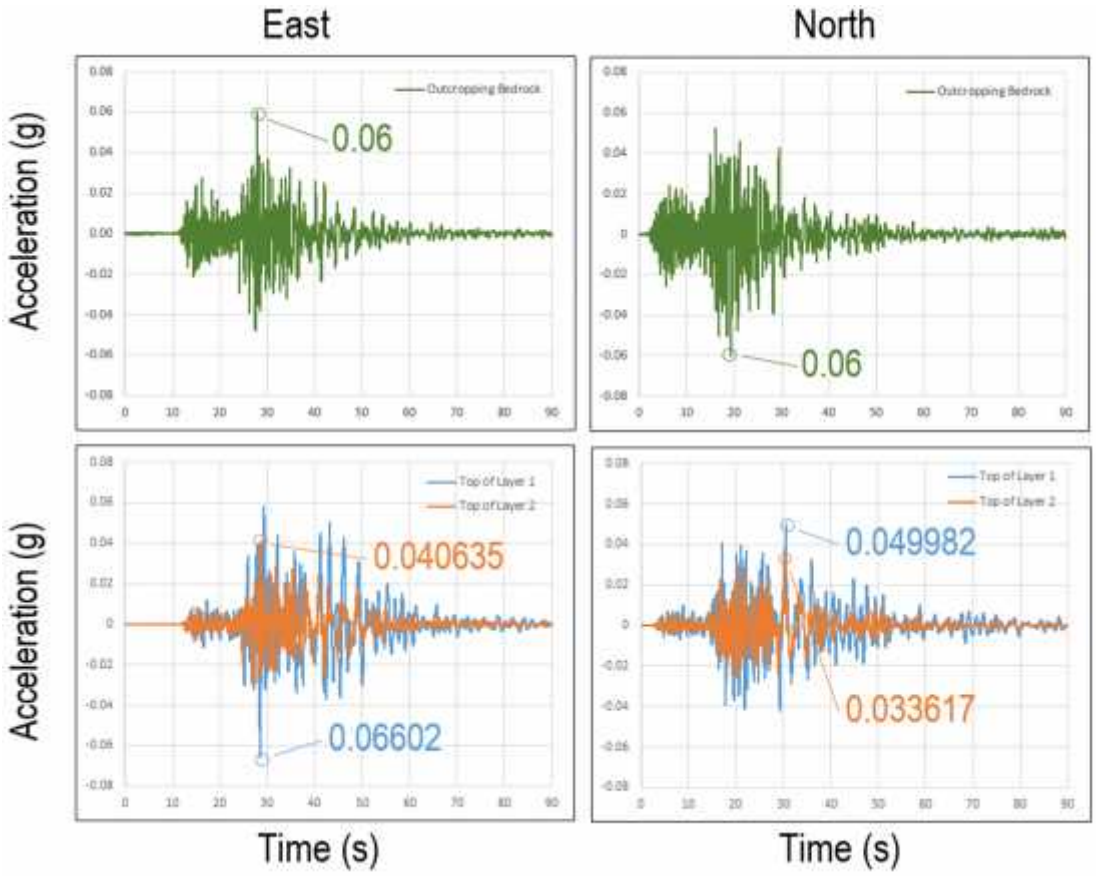

Figure 11 Sumandak: Time series of bedrock motion and soil layers due to Bintulu Earthquake on 1 May 2004 scaled to 0.06g

Amplification of Peak Ground Acceleration (A_{pga})

Table 8 Sumandak: Amplification of peak ground acceleration (A_{pga}) due to Bintulu earthquake on 1 May 2004 scaled to 0.06g

	East	North
Layer 1	1.10	0.83
Layer 2	0.68	0.56

After the bedrock acceleration time history is scaled to 0.06g, which is about 40 times of the original bedrock acceleration, the PGA is no longer amplified except on top of layer 1 in the east direction in which the amplification of PGA is 1.10. The drastic drop in the amplification of PGA can be explained by the nonlinearity of site

response. The response of the soil will be nonlinear under strong shaking. The shear modulus and damping of soil are strain dependent. Thus, the larger strains, caused by strong shaking, decrease the effective shear moduli and increase the damping. This reduces the amplification of PGA accordingly.

Besides, similar trend is observed in which the amplification of PGA on top of layer 1 is higher than the top of layer 2 because of the impedance contrast of shear wave velocities between the two layers as explained in chapter 4.1.2. Figure 12 and Figure 13 show the maximum PGA vs. depth for the east and north direction.

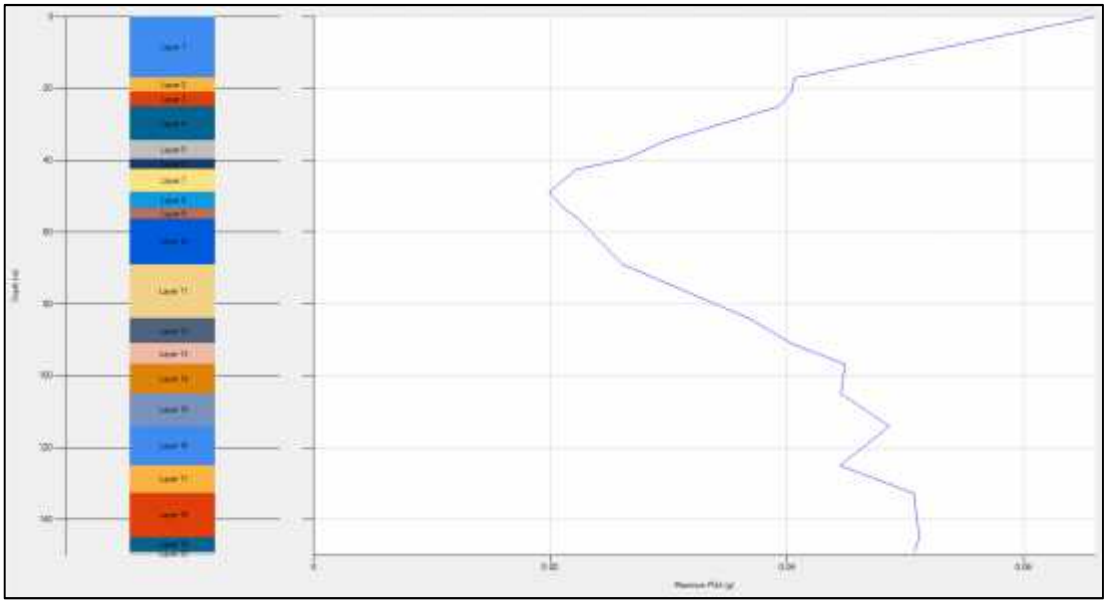

Figure 12 Sumandak: Graph of maximum peak ground acceleration vs. depth in the east direction (scaled to 0.06g)

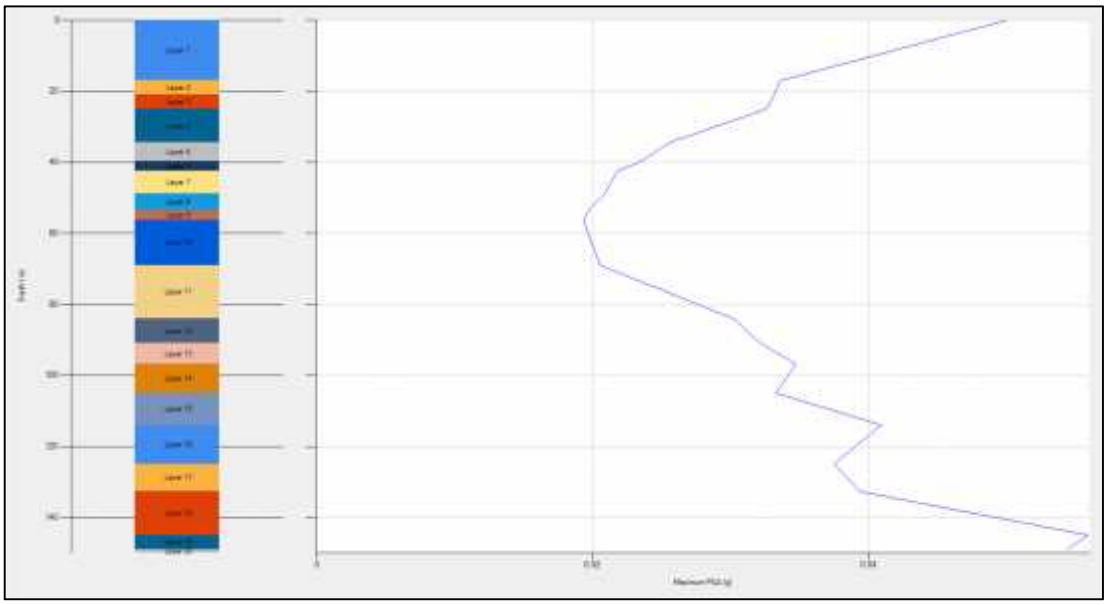

Figure 13 Sumandak: Graph of maximum peak ground acceleration vs. depth in the north direction (scaled to 0.06g)

Fourier Spectra, Response Spectra and Amplification of Response Spectra (F_a)

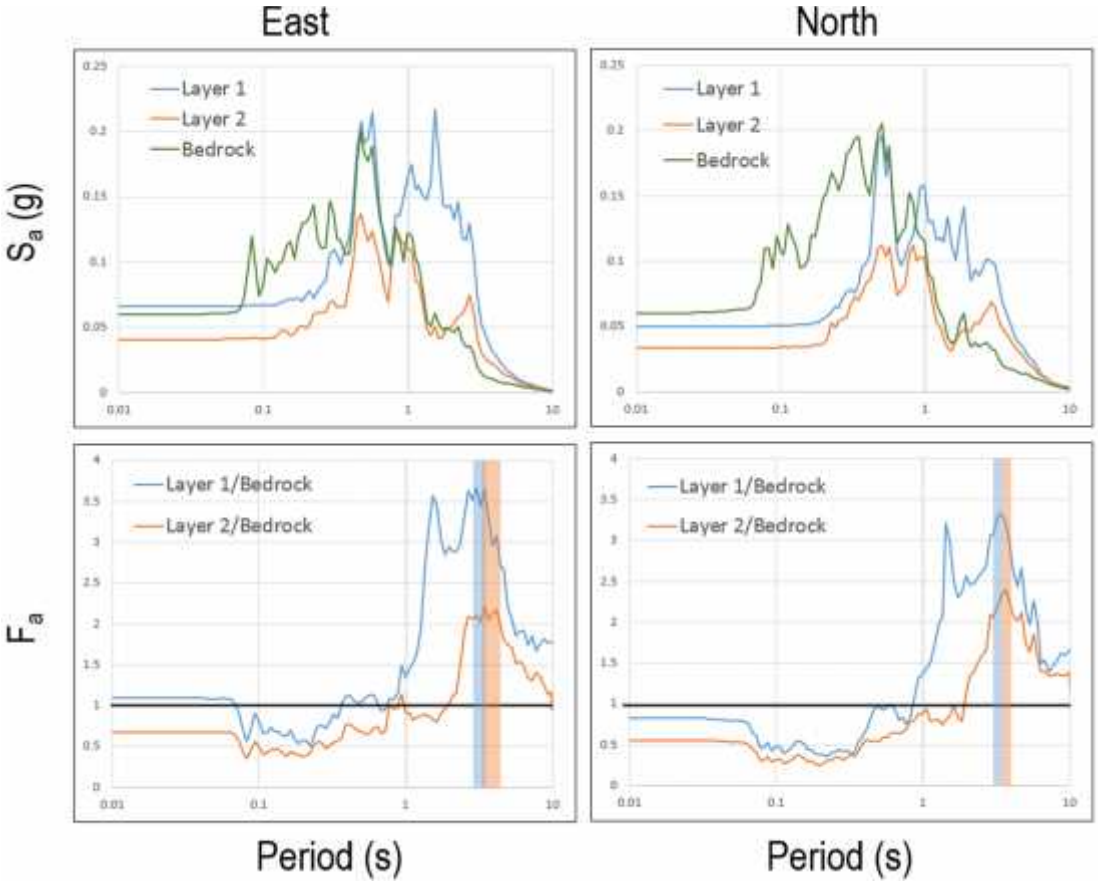

Figure 14 Sumandak: Fourier spectra, response spectra and amplification of response spectra (F_a) due to Bintulu Earthquake on 1 May 2004 scaled to 0.06g

From the graph of amplification of response spectra, it can be seen that the amplification factors are remarkably reduced in the scaled (stronger) earthquake,

although the amplification factor is above 2 for layer 1 over a wide frequency band of engineering interest. The reduction in amplification with increased intensity of shaking is due to the nonlinear stress-strain response of the soil, resulting from reduced effective shear moduli and increased damping as explained in the discussion of amplification of PGA.

Furthermore, it is observed that the peak spectral acceleration ranges between periods of 3.04 second to 3.66 second for the both soil layer in the both directions. These values correspondent to the fundamental site period of site Sumandak which is 3.29 second. These findings are in the interest of engineering where the design of structures should avoid the range of these periods as the amplification factor of 3.67 is associated with PGA of 0.06g which is significant enough to damage the platforms on site.

Table 9 Sumandak: Peak spectral amplification ($F_{a,p}$) and amplification factor (F_a) at 0.06g earthquake

Layer	F_a	East	North
Layer 1/ Bedrock	$F_{a,p}$	3.67 @ 3.04125s	3.33 @ 3.44375s
	F_a (0.1-0.5s)	0.77	0.51
	F_a (0.4-2.0s)	1.77	1.53
Layer 2/ Bedrock	$F_{a,p}$	2.22 @ 3.44375s	2.41 @ 3.66456s
	F_a (0.1-0.5s)	0.52	0.36
	F_a (0.4-2.0s)	0.85	0.77

The amplification factors, F_a (0.1-0.5s) and F_a (0.4-2.0s) are obtained as the average ratios of Fourier spectra over two period ranges, 0.1 to 0.5s and 0.4 to 2.0s. The period ranges correspond to those used for obtaining average amplification factors for the NEHRP Provisions (BSSC, 2003).

As shown in Table 9, all the amplification factors, F_a (0.1-0.5s) and F_a (0.4-2.0s) are less than 1 except for F_a (0.4-2.0s) on top of layer 1 in the east and north direction. The amplification factor for seismic wave period ranging from 0.4s to 2.0s are between 1.77 and 1.53, which are much less than the values of 3.66 and 3.55 for the unscaled earthquake counterparts. However, due to the stronger earthquake (PGA= 0.06g), this frequency band should be taken into account in the design of structure.

The peak acceleration at the surface is 0.06g. Therefore, it should be noted that the amplification factors are associated with fairly low levels of earthquake (PGA= 0.06g) shaking although it is significantly higher than the very low levels of earthquake shaking (0.0015g) in chapter 4.1.2.

4.1.4 Discussion

For the unscaled earthquake with PGA of about 0.0015g, the amplification factors are high, around 3.6 (period 0.4s-2.0s) and 2.35 (period 0.1s-0.5s). However, these amplification factors are associated with very low levels of earthquake shaking which will hardly bring harm to the structure on site.

In contrast, for the scaled earthquake with PGA of about 0.06g, the amplification factors are around 1.6 (period 0.4s-2.0s) and 0.6 (period 0.1s-0.5s). The drastically reduced amplification factors are caused by the nonlinear behaviour of soils which has been explained in chapter 4.1.3. On the other hand, the peak spectral amplification is around 3.5 at period ranging from 3.04s to 3.44s which correspond to the fundamental site period of 3.29s. These amplification factors should be taken into account during the design of structure because they are associated with PGA of 0.06g which is significant enough to damage the platforms on site, especially if the seismic waves are amplified.

4.2 Kumang

4.2.1 Soil Profile

Table 10 Kumang: Soil layers and their properties

Layer	Layer Name	Thickness (m)	Unit Weight (kN/m^3)	Shear Velocity (m/s)
1	Very Soft CLAY	1	17.81	39.42
2	Loose SAND	2.5	17.81	90.02
3	Firm CLAY	1.8	17.81	159.91
4	Loose to Medium Dense SAND	1.9	17.81	146.71
5	Stiff CLAY	3.6	17.81	198.11
6	Firm to Stiff CLAY	21.1	17.81	221.36
7	Medium Dense SAND	2.1	17.81	235.44
8	Stiff to Very Stiff CLAY	10.9	17.81	251.23
9	Very Stiff CLAY	6.3	17.81	260.78
10	Loose to Medium Dense SILT	4.6	17.81	226.18
11	Very Stiff CLAY	4.3	17.81	265.72
12	Medium Dense SILT	7.9	17.81	235.44
13	Very Stiff CLAY	25.8	17.81	277.02
14	Dense SAND	7.4	17.81	245.23
15	Hard SILT	8.7	17.81	291.86
16	Hard CLAY	12.1	17.81	291.86
17	Dense SAND	4	17.81	245.23
18	Hard CLAY	15.4	17.81	298.17
19	Hard CLAY	4.7	17.81	303.38
20	Dense SAND	5.9	17.81	245.23
21	Hard CLAY	2.5	17.81	314.22
22	Dense SAND	21.5	17.81	245.23
23	Hard SILT	4	17.81	320.74

Fundamental site period

$$T_S = 4 \sum \frac{H_i}{V_s} = 4 \times 0.74756 = 2.99s$$

where H_i = thickness of ith soil layer

V_{si} = V_s of ith layer (Kramer, 1996)

4.2.2 Seismic Ground Response based on Bintulu Earthquake on 1 May 2004

Ground Acceleration Time History

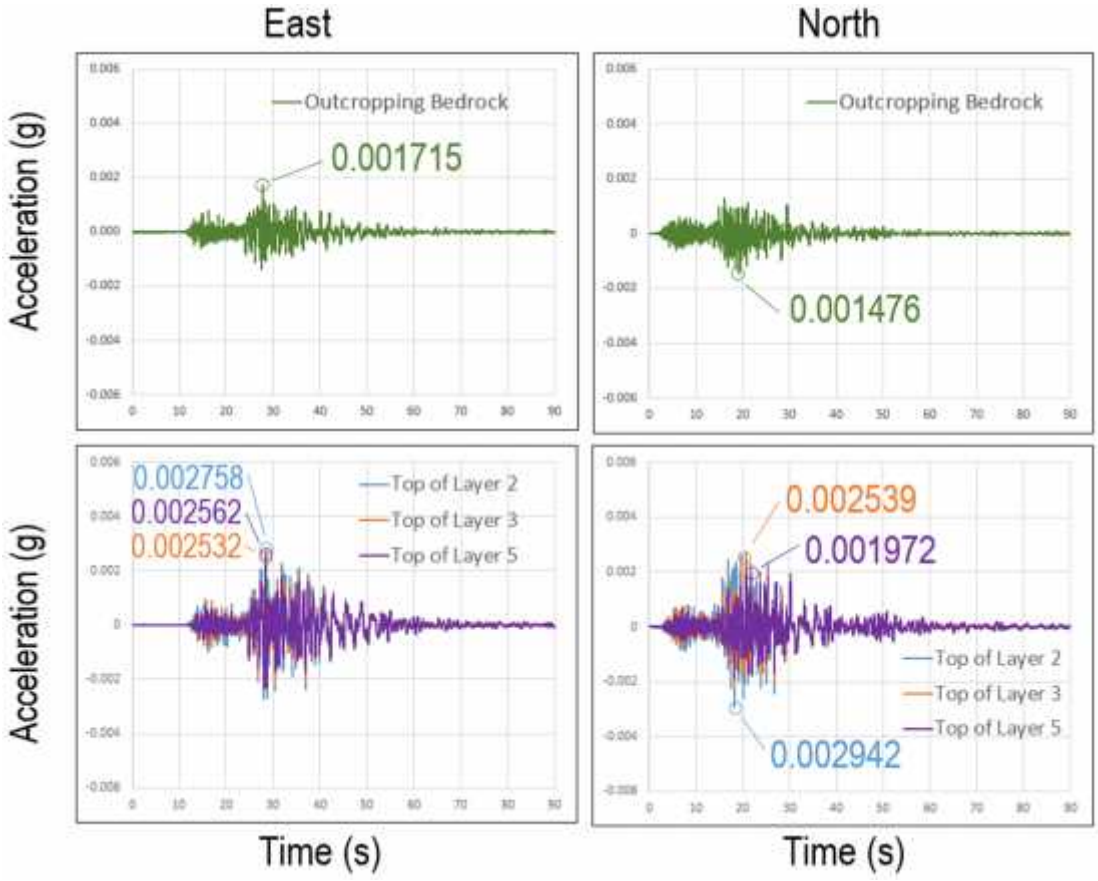

Figure 15 Kumang: Time series of bedrock motion and soil layers due to Bintulu Earthquake on 1 May 2004

Amplification of Peak Ground Acceleration (A_{pga})

Table 11 Kumang: Amplification of peak ground acceleration (A_{pga}) due to Bintulu earthquake on 1 May 2004

	East	North
Layer 2	1.61	1.99
Layer 3	1.48	1.72
Layer 5	1.49	1.34

From Table 10 above, it should be noted that the thicknesses of layer 2, 3 and 5 are 2.5m, 1.8m and 3.6m respectively and they have a shear wave velocity of 90.02m/s, 159.91m/s and 198.11m/s accordingly. According to Modified Malaysian Site Class (D'Appolonia, 2009), layer 2 is classified as 'very soft normally consolidated clay', layer 3 is classified as 'soft to firm soil' and layer 5 is classified as 'stiff to very stiff soil'.

The amplification of PGA at the top of layer 2 in the east and north direction are 1.61 and 1.99 respectively. On the other hand, for layer 3 and layer 5 in the both direction, the amplification of PGA ranges from 1.34 to 1.72. The impedance contrast of shear wave velocities between the boundaries of layer 2 and layer 3 amplifies the incoming seismic waves significantly resulting in noticeable higher A_{pga} in layer 2 than layer 3. Figure 16 and Figure 17 below show the maximum PGA vs. depth in the east direction and north direction.

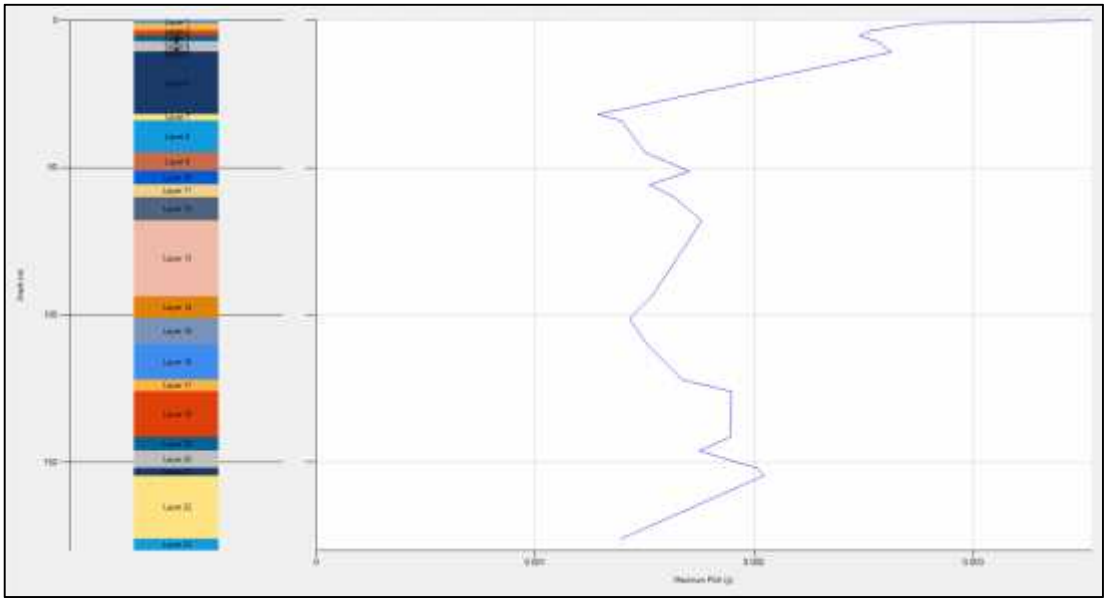

Figure 16 Kumang: Graph of maximum peak ground acceleration vs. depth in the east direction

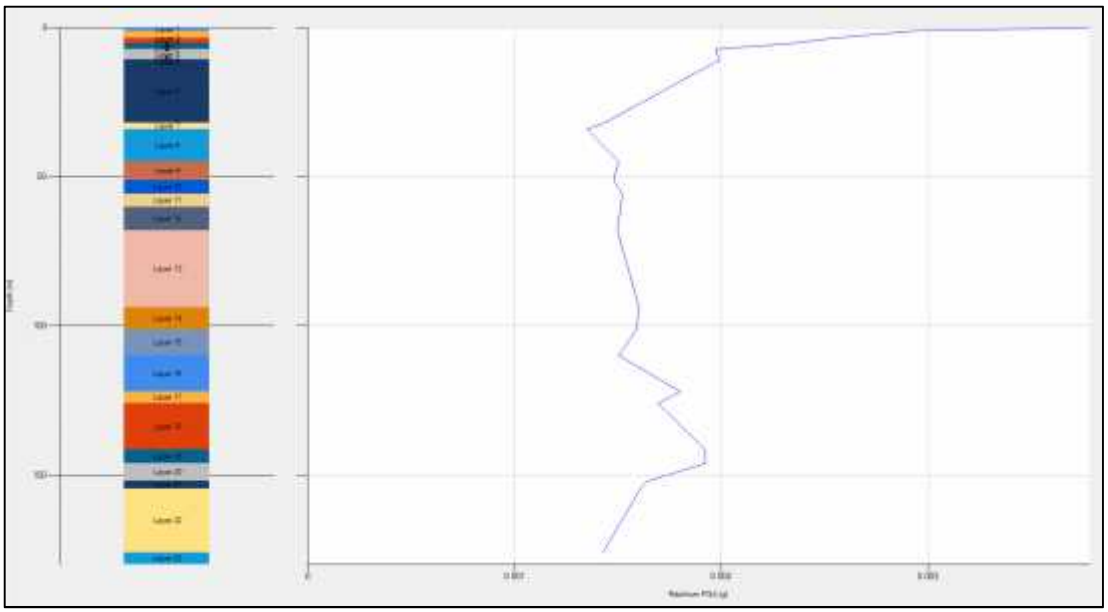

Figure 17 Kumang: Graph of maximum peak ground acceleration vs. depth in the north direction

Fourier Spectra, Response Spectra and Amplification of Response Spectra (F_a)

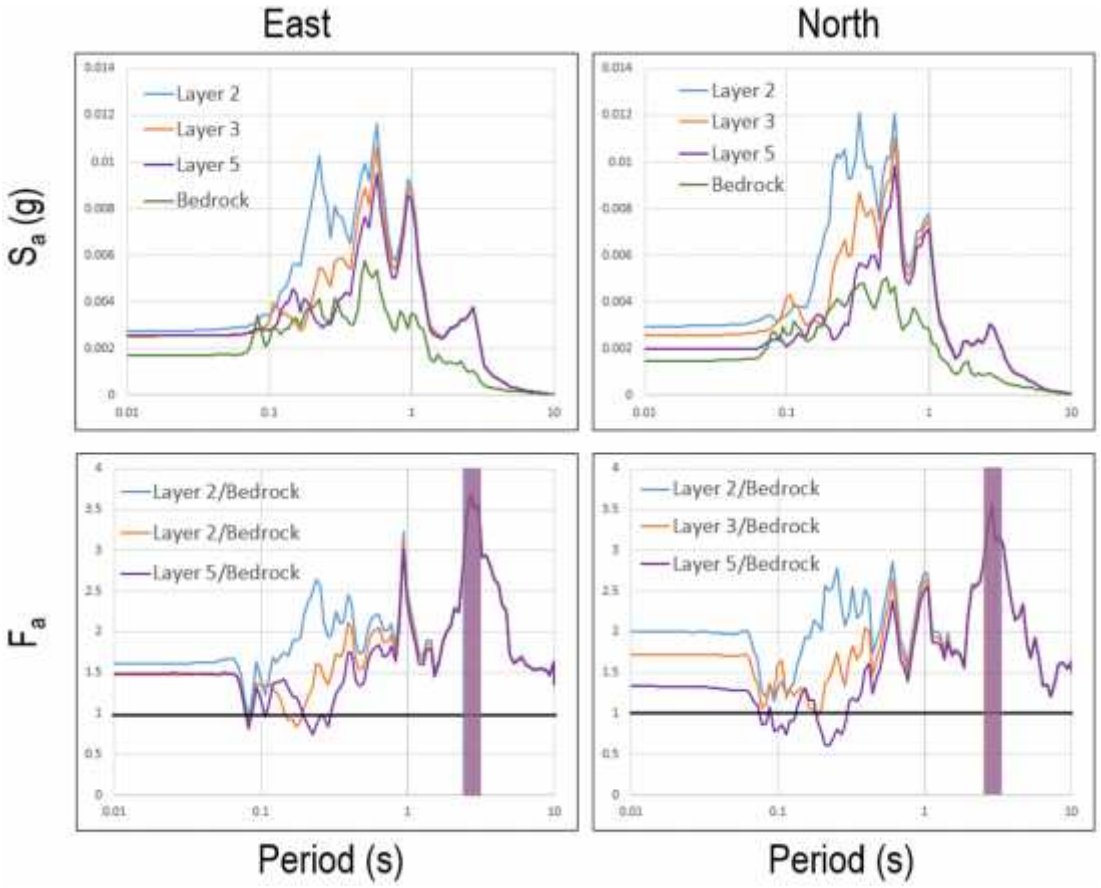

Figure 18 Kumang: Fourier spectra, response spectra and amplification of response spectra (F_a) due to Bintulu Earthquake on 1 May 2004

It can be seen from the graph of amplification of response spectra above that all layers are amplified for almost the whole range of period in both direction except for period between 0.1s and 0.3s of layer 5 in the north direction.

On the other hand, all the peak spectral acceleration happens at period 2.6858s and 2.858s in the east and north direction respectively. They are close to the fundamental site period of 2.99s. The peak spectral acceleration factors range from 3.54 to 3.71.

Table 12 Kumang: Peak spectral amplification ($F_{a,p}$) and amplification factor (F_a) at 0.0015g earthquake

Layer	F_a	East	North
Layer 2/ Bedrock	$F_{a,p}$	3.71 @ 2.6858s	3.57 @ 2.858s
	F_a (0.1-0.5s)	1.97	2.02
	F_a (0.4-2.0s)	2.05	2.12
Layer 3/ Bedrock	$F_{a,p}$	3.69 @ 2.6858s	3.56 @ 2.858s
	F_a (0.1-0.5s)	1.40	1.48
	F_a (0.4-2.0s)	1.94	2.01
Layer 5/ Bedrock	$F_{a,p}$	3.67 @ 2.6858s	3.54 @ 2.858s
	F_a (0.1-0.5s)	1.20	1.05
	F_a (0.4-2.0s)	1.82	1.88

The amplification factors, F_a (0.1-0.5s) and F_a (0.4-2.0s) are obtained as the average ratios of Fourier spectra over two period ranges, 0.1 to 0.5s and 0.4 to 2.0s. The period ranges correspond to those used for obtaining average amplification factors for the NEHRP Provisions (BSSC, 2003).

The amplification factors for period between 0.4s and 2.0s range from 1.82 to 2.12 for all selected layers. The peak ground acceleration of the input motion is only about 0.0015g, so the amplification factors are associated with very low levels of earthquake shaking.

4.2.3 Seismic Ground Response based on Bintulu Earthquake on 1 May 2004 scaled to 0.06g

Ground Acceleration Time History

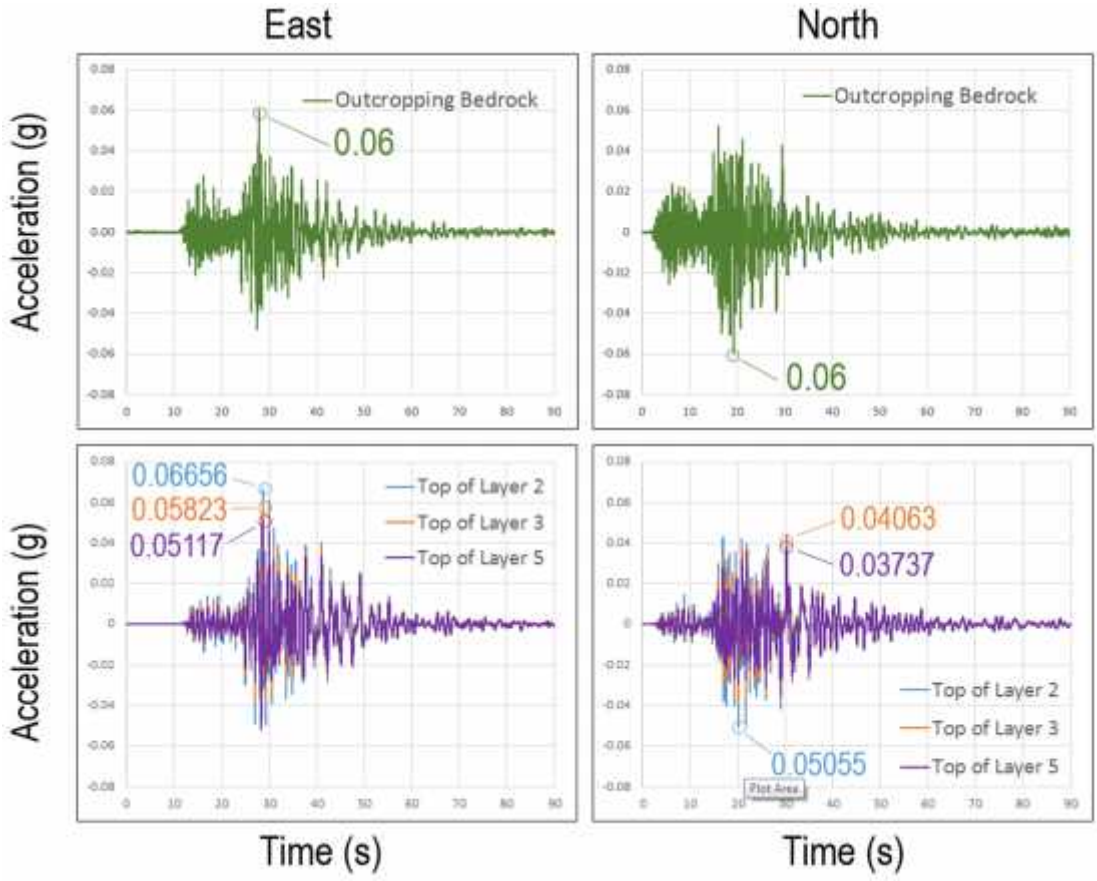

Figure 19 Kumang: Time series of bedrock motion and soil layers due to Bintulu Earthquake on 1 May 2004 scaled to 0.06g

Amplification of Peak Ground Acceleration (A_{pga})

Table 13 Kumang: Amplification of peak ground acceleration (A_{pga}) due to Bintulu earthquake on 1 May 2004 scaled to 0.06g

	East	North
Layer 2	1.11	0.84
Layer 3	0.97	0.68
Layer 5	0.85	0.62

After the bedrock acceleration time history is scaled to 0.06g, which is about 40 times of the original bedrock acceleration, the PGA is no longer amplified except on top of layer 2 in the east direction in which the amplification of PGA is 1.11. The

drastic drop in the amplification of PGA can be explained by the nonlinearity of site response as discussed in chapter 4.1.3.

Besides, similar trend is observed in which the amplification of PGA on top of layer 1 is higher than the top of layer 2 because of the impedence contrast of shear wave velocities between the two layers as explained in chapter 4.1.2.

Figure 20 and Figure 21 below show the maximum PGA vs. depth in the east direction and north direction.

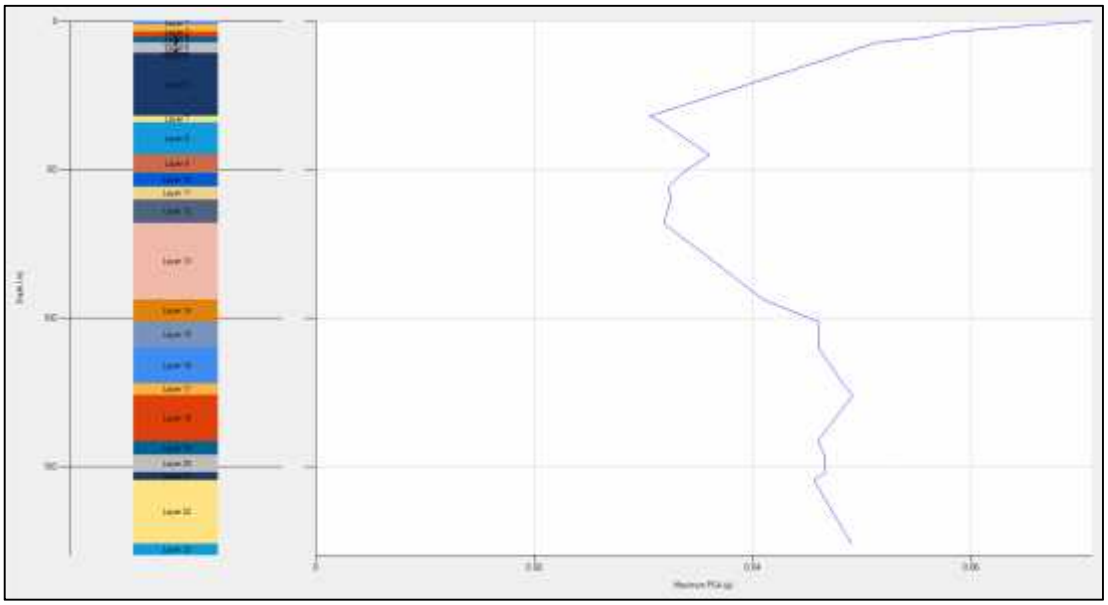

Figure 20 Kumang: Graph of maximum peak ground acceleration vs. depth in the east direction (scaled to 0.06g)

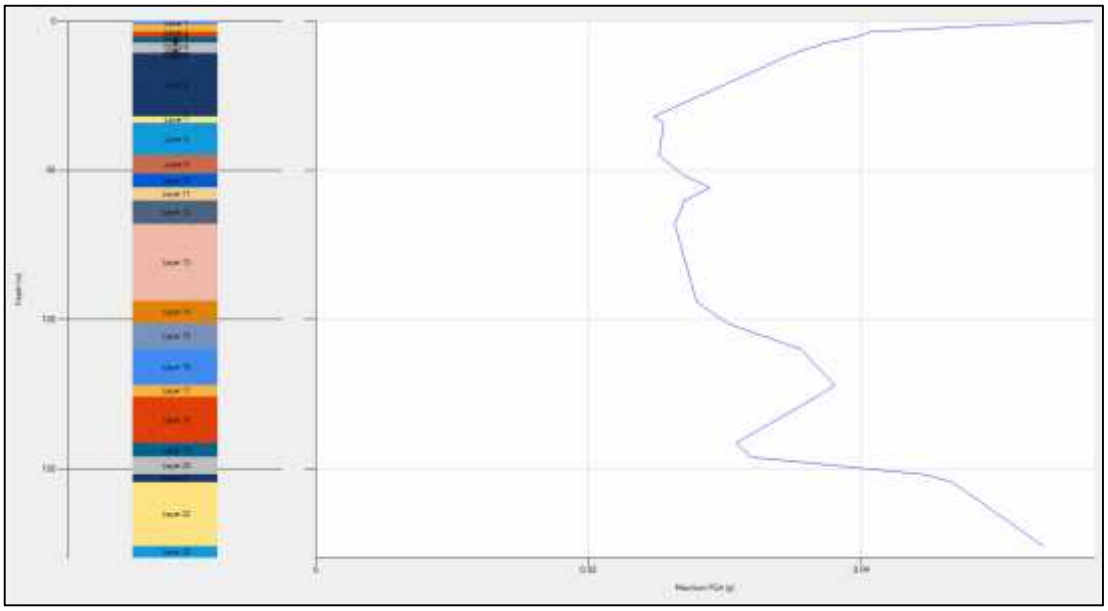

Figure 21 Kumang: Graph of maximum peak ground acceleration vs. depth in the north direction (scaled to 0.06g)

Fourier Spectra, Response Spectra and Amplification of Response Spectra (F_a)

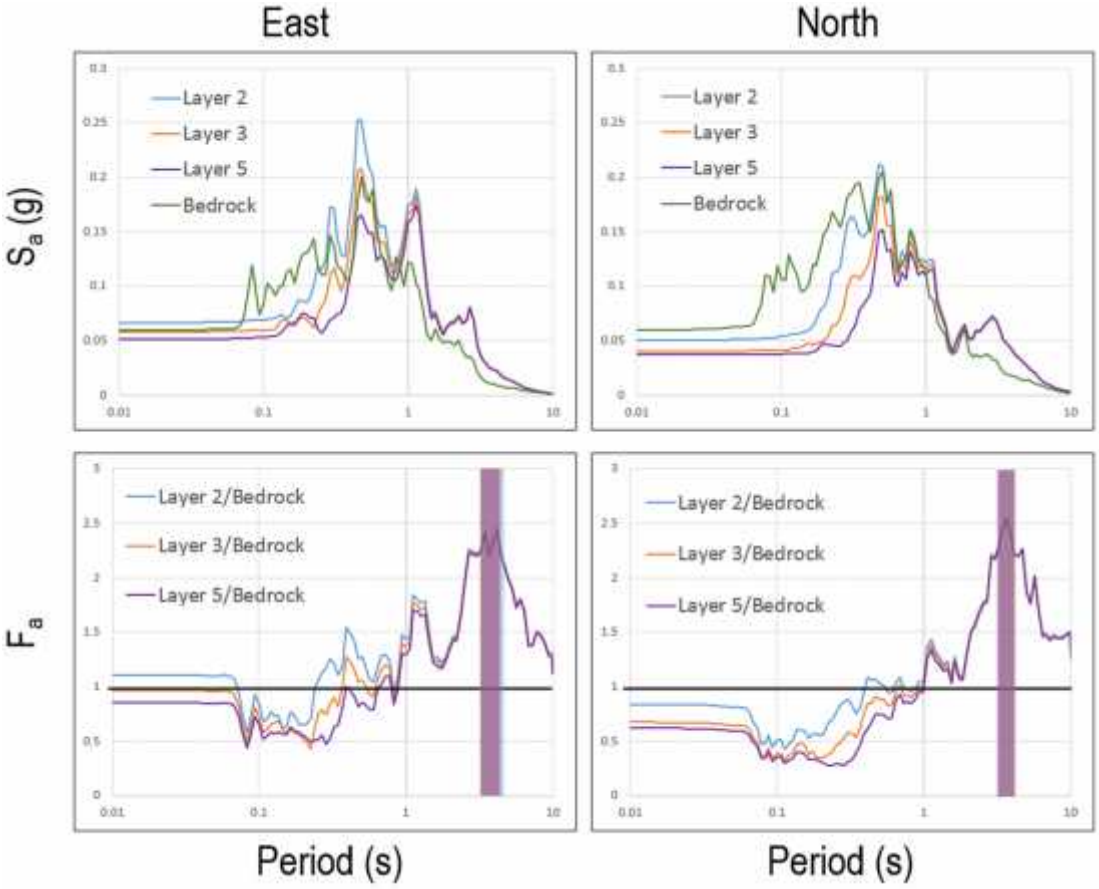

Figure 22 Kumang: Fourier spectra, response spectra and amplification of response spectra (F_a) due to Bintulu Earthquake on 1 May 2004 scaled to 0.06g

From the graph of amplification of response spectra, it can be seen that the amplification factors are remarkably reduced in the scaled (stronger) earthquake, although the amplification factor is above 2 for all layers over a wide frequency band of engineering interest. The reduction in amplification with increased intensity of shaking is due to the nonlinear stress-strain response of the soil, resulting from reduced effective shear moduli and increased damping as explained in chapter 4.1.3 above.

Furthermore, it is observed that the peak spectral amplification happens at period 4.15s in the east direction and 3.66 in the north direction. These periods are far from the fundamental site period of 2.99 second calculated in chapter 4.2.1. The peak spectral amplification factors of 2.45 at period 4.15s and 2.54 at period 3.66s are in the interest of engineering where the design of structures should avoid the range of these periods as these amplification factors are associated with PGA of 0.06g which is significant enough to damage the platforms on site.

Table 14 Kumang: Peak spectral amplification ($F_{a,p}$) and amplification factor (F_a) at 0.06g earthquake

Layer	F_a	East	North
Layer 2/ Bedrock	$F_{a,p}$	2.46 @ 4.14955s	2.55 @ 3.66456s
	F_a (0.1-0.5s)	0.96	0.72
	F_a (0.4-2.0s)	1.36	1.13
Layer 3/ Bedrock	$F_{a,p}$	2.45 @ 4.14955s	2.54 @ 3.66456s
	F_a (0.1-0.5s)	0.76	0.52
	F_a (0.4-2.0s)	1.27	1.06
Layer 5/ Bedrock	$F_{a,p}$	2.44 @ 4.14955s	2.53 @ 3.66456s
	F_a (0.1-0.5s)	0.64	0.40
	F_a (0.4-2.0s)	1.17	0.99

The amplification factors, F_a (0.1-0.5s) and F_a (0.4-2.0s) are obtained as the average ratios of Fourier spectra over two period ranges, 0.1 to 0.5s and 0.4 to 2.0s. The period ranges correspond to those used for obtaining average amplification factors for the NEHRP Provisions (BSSC, 2003).

As shown in Table 14, F_a (0.1-0.5s) are less than 1 in the both direction. F_a (0.4-2.0s) ranges from 1.17 to 1.36 in the east direction and 0.99 to 1.13 in the north direction. These values are much less than the F_a (0.4-2.0s) of 1.82 in the east direction of the unscaled earthquake counterpart. Lastly, it should be noted that these amplification factors are associated with fairly low levels of earthquake (PGA= 0.06g).

4.2.4 Discussion

For the discussion, only the top of layer 5 will be considered because layer 5 extends from the depth of 7.2m to 10.8m. The soils at depth shallower than 7.2m shall not bring significant influence to the structure response due to the relatively deep piling in offshore structures.

For the unscaled earthquake with PGA of about 0.0015g, the amplification factors are around 1.85 (period 0.4s-2.0s) and 1.1 (period 0.1s-0.5s). However, these amplification factors are associated with very low levels of earthquake shaking which will hardly bring harm to the structure on site.

In contrast, for the scaled earthquake with PGA of about 0.06g, the amplification factors are around 1.1 (period 0.4s-2.0s) and 0.5 (period 0.1s-0.5s). The drastically reduced amplification factors are caused by the nonlinear behaviour of soils which has been explained in chapter 4.1.3. On the other hand, the peak spectral acceleration is around 2.5 at period ranging from 3.66s to 4.15s which are deviated from the fundamental site period of 2.99s. These amplification factors should be taken into account during the design of structure because they are associated with PGA of 0.06g which is significant enough to damage the platforms on site, especially if the seismic waves are amplified.

4.3 Laho

4.3.1 Soil Profile

Table 15 Laho: Soil layers and their properties

Layer	Layer Name	Thickness (m)	Unit Weight (kN/m^3)	Shear Velocity (m/s)
1	Stiff to very stiff CLAY	15	18.31	173.06
2	Stiff to very stiff CLAY	15	18.11	193.98
3	Stiff to very stiff CLAY	20	18.61	208.82
4	Stiff to very stiff CLAY	20	18.41	225.04
5	Very stiff to hard CLAY	10	18.31	231.81
6	Very stiff to hard CLAY	10	18.31	220.34
7	Medium dense to dense SAND	5	18.71	198.71
8	Medium dense to dense SAND	10	18.81	265.51
9	Medium dense to dense SAND	10	18.81	265.51
10	Very stiff to hard CLAY	10	18.31	220.34
11	Very stiff to hard CLAY	15	18.01	242.29

Fundamental site period

$$T_S = 4 \sum \frac{H_i}{V_S} = 4 \times 0.64496 = 2.58s$$

where H_i = thickness of ith soil layer

V_{si} = V_s of ith layer (Kramer, 1996)

4.3.2 Seismic Ground Response based on Sumatra Earthquake on 28 March 2005

Ground Acceleration Time History

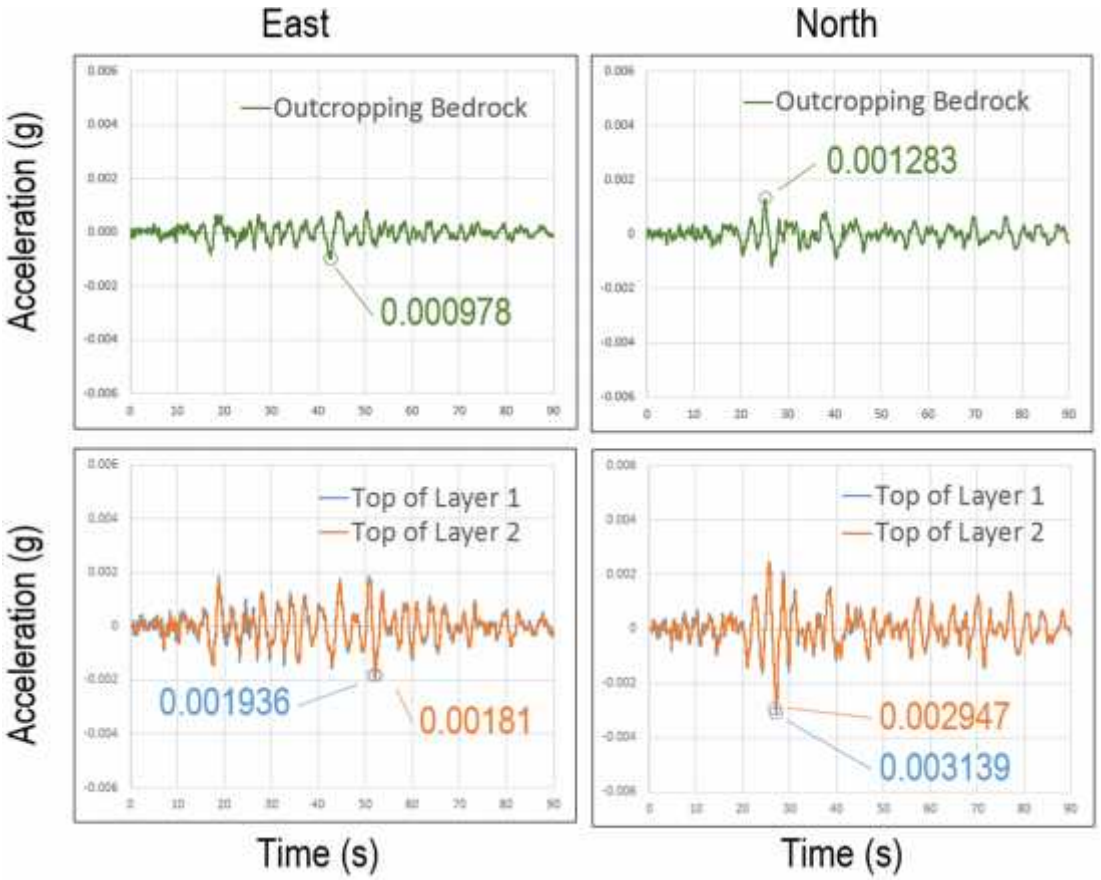

Figure 23 Laho: Time series of bedrock motion and soil layers due to Sumatra earthquake on 28 March 2005

Amplification of Peak Ground Acceleration (A_{pga})

Table 16 Laho: Amplification of peak ground acceleration (A_{pga}) due to Sumatra earthquake on 28 March 2005

	East	North
Layer 1	1.98	2.45
Layer 2	1.85	2.30

The amplification of PGA at the top of layer 1 and layer 2 in the east direction are 1.98 and 1.85 respectively and in the north direction are 2.45 and 2.30 respectively. Layer 1 and layer 2 are both 15m thick 'stiff to very stiff clay' having shear wave velocities of 173.06m/s and 193.98m/s respectively. The relatively small difference in shear wave velocities between the two layers caused the A_{pga} difference between

layer 1 and 2 to be small as well. Figure 24 and Figure 25 below show the maximum PGA vs. depth in the east direction and north direction.

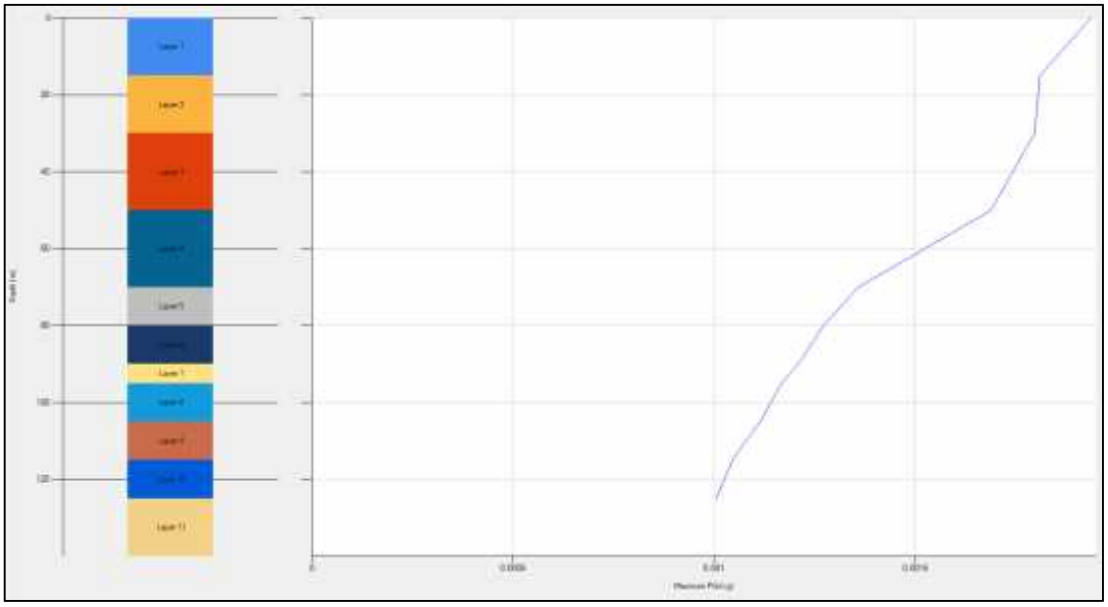

Figure 24 Laho: Graph of maximum peak ground acceleration vs. depth in the east direction

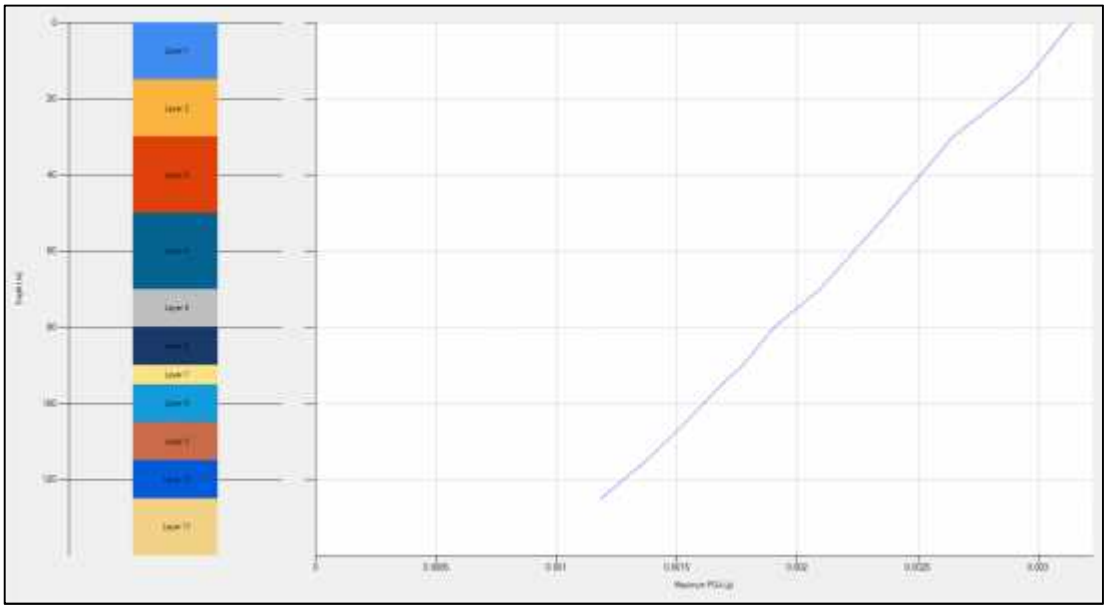

Figure 25 Laho: Graph of maximum peak ground acceleration vs. depth in the north direction

Fourier Spectra, Response Spectra and Amplification of Response Spectra (F_a)

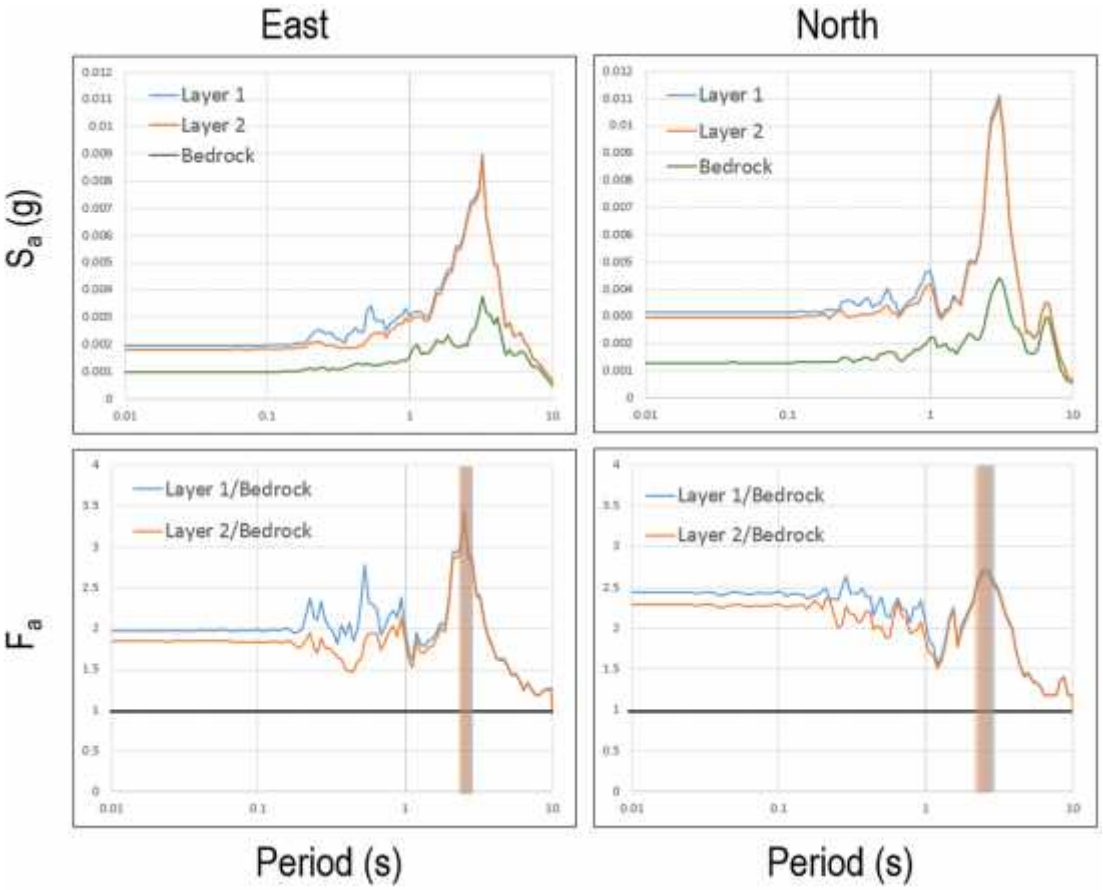

Figure 26 Laho: Fourier spectra, response spectra and amplification of response spectra (F_a) due to Sumatra Earthquake on 28 March 2005

It can be seen from the graph of amplification of response spectra that layer 1 and layer 2 are amplified for the whole range of period in both direction. In the both direction, the peak spectral amplification for the both layers happens at period 2.52s which is very close to the fundamental site period of 2.58s although the amplification is around 3.4 in the east direction and 2.7 in the north direction.

Table 17 Laho: Peak spectral acceleration ($F_{a,p}$) and amplification factor (F_a) at 0.0011g earthquake

Layer	F_a	East	North
Layer 1/ Bedrock	$F_{a,p}$	3.44 @ 2.52396s	2.73 @ 2.52396s
	F_a (0.1-0.5s)	2.04	2.41
	F_a (0.4-2.0s)	2.10	2.12
Layer 2/ Bedrock	$F_{a,p}$	3.37 @ 2.52396s	2.68 @ 2.52396s
	F_a (0.1-0.5s)	1.75	2.20
	F_a (0.4-2.0s)	1.86	1.98

The amplification factors, F_a (0.1-0.5s) and F_a (0.4-2.0s) are obtained as the average ratios of Fourier spectra over two period ranges, 0.1 to 0.5s and 0.4 to 2.0s. The period ranges correspond to those used for obtaining average amplification factors for the NEHRP Provisions (BSSC, 2003). The amplification factors are shown in the table above. The peak acceleration at the surface is only about 0.0011g, so the amplification factors are associated with very low levels of earthquake shaking.

4.3.3 Seismic Ground Response based on Sumatra Earthquake on 28 March 2005 scaled to 0.06g

Ground Acceleration Time History

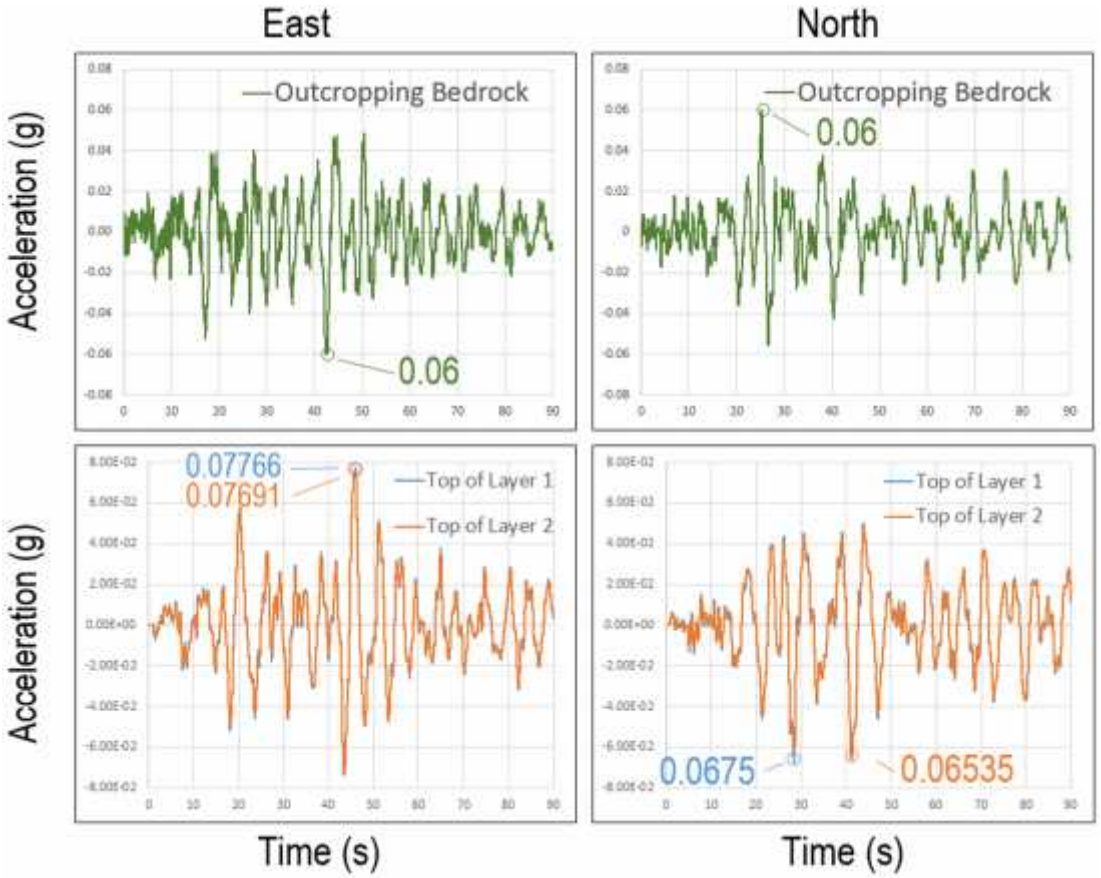

Figure 27 Laho: Time series of bedrock motion and soil layers due to Sumatra earthquake on 28 March 2005 scaled to 0.06g

Amplification of Peak Ground Acceleration (A_{pga})

Table 18 Laho: Amplification of peak ground acceleration (A_{pga}) due to Sumatra earthquake on 28 March 2005 scaled to 0.06g

	East	North
Layer 1	1.29	1.12
Layer 2	1.28	1.09

After the bedrock acceleration is scaled to 0.06g, which is about 54 times of the original bedrock acceleration, the PGA is only slightly amplified. The drastic drop in the A_{pga} can be explained by the nonlinearity behaviour of soil as explained in chapter 4.1.3. The A_{pga} on top of layer 1 is only slightly higher than layer 2 due to their very similar shear wave velocities.

It should be noted that the A_{pga} in Sumandak and Kumang is less than one in scaled earthquake but more than 1 in Laho. The difference might be caused by the different input ground motion. It is noticeable that the input ground motion of Sumatra earthquake on 28 March 2005 has a much longer zero-crossing period than the Bintulu earthquake on 1 May 2004.

Figure 28 and Figure 29 below show the maximum PGA vs. depth in the east direction and north direction.

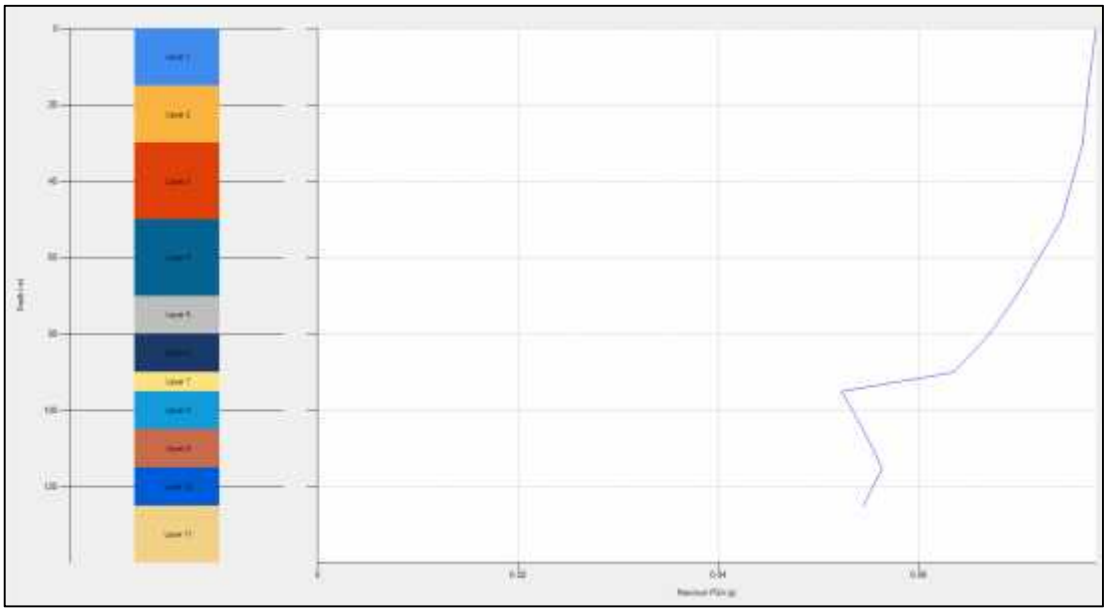

Figure 28 Laho: Graph of maximum peak ground acceleration vs. depth in the east direction (scaled to 0.06g)

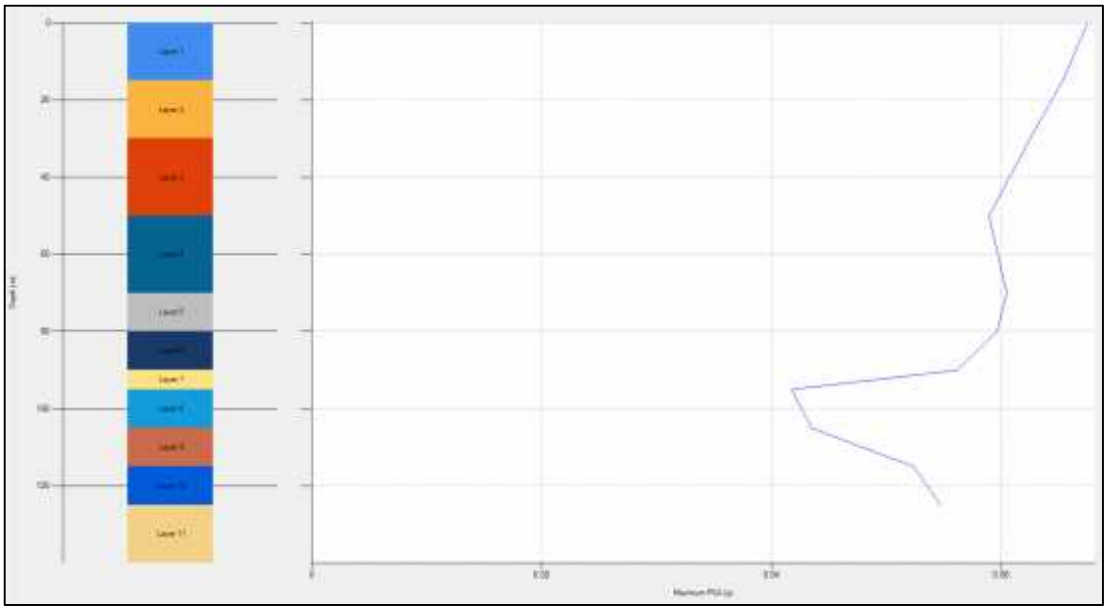

Figure 29 Laho: Graph of maximum peak ground acceleration vs. depth in the north direction (scaled to 0.06g)

Fourier Spectra, Response Spectra and Amplification of Response Spectra (F_a)

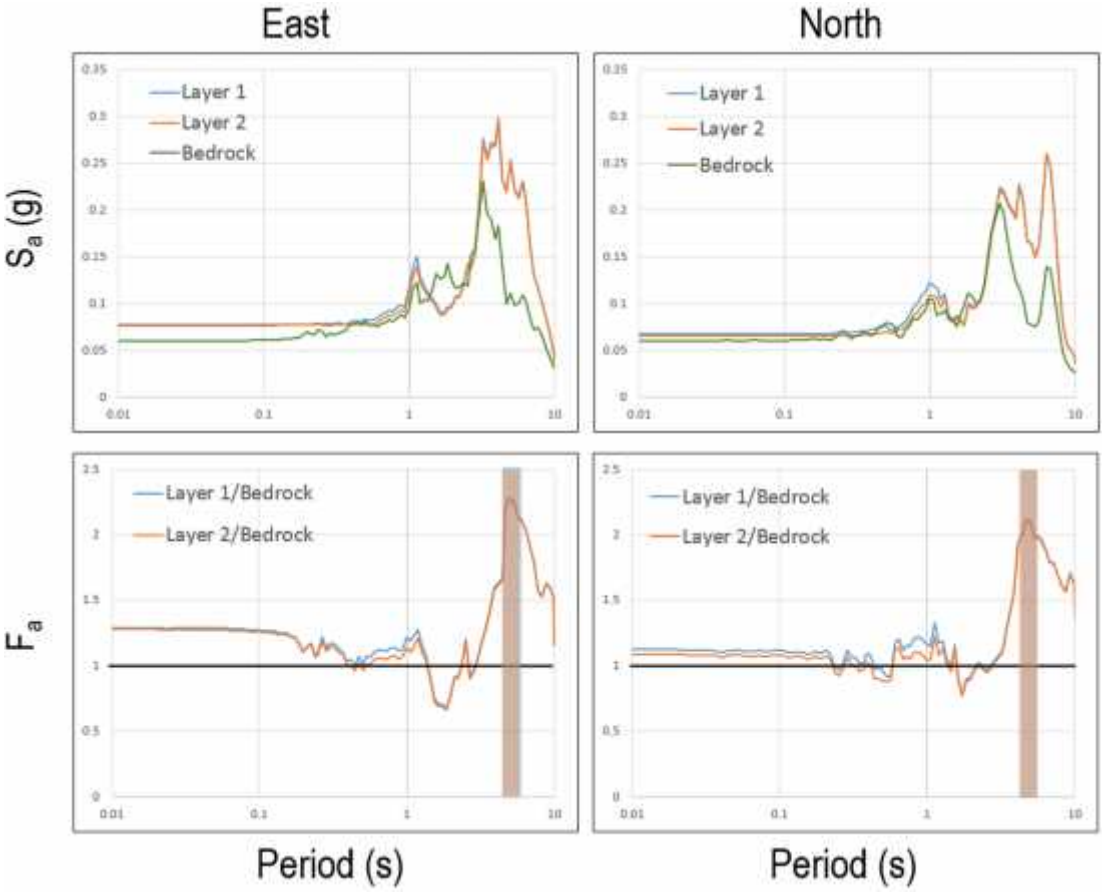

Figure 30 Laho: Fourier spectra, response spectra and amplification of response spectra (F_a) due to Sumatra Earthquake on 28 March 2005 scaled to 0.06g

Similar to site Sumandak and Kumang, the amplification factors are remarkably reduced in the scaled to stronger earthquake (0.06g) due to the nonlinearity behaviour of soil. However, it should be noted that the F_a of high frequency waves with period less than 0.3s are more than 1. In other words, the high frequency waves of site Laho are amplified. Conversely, in both the case studies of Sumandak and Kumang with earthquake scaled to 0.06g, these high frequency seismic waves are mostly dampened. This is probably caused by the different seismic input motion which has varying characteristics and properties.

Besides, the peak spectral acceleration is 2.28 at period 5s in the east direction and 2.11 at period 4.7s in the north direction. They are far from the fundamental site period of 2.58s.

Table 19 Laho: Peak spectral amplification ($F_{a,p}$) and amplification factor (F_a) at 0.06g earthquake

Layer	F_a	East	North
Layer 1/ Bedrock	$F_{a,p}$	2.28 @ 5s	2.11 @ 4.70s
	F_a (0.1-0.5s)	1.17	1.07
	F_a (0.4-2.0s)	1.03	1.08
Layer 2/ Bedrock	$F_{a,p}$	2.27 @ 5s	2.10 @ 4.70s
	F_a (0.1-0.5s)	1.15	1.02
	F_a (0.4-2.0s)	0.99	1.01

The amplification factors, F_a (0.1-0.5s) and F_a (0.4-2.0s) are obtained as the average ratios of Fourier spectra over two period ranges, 0.1 to 0.5s and 0.4 to 2.0s. The period ranges correspond to those used for obtaining average amplification factors for the NEHRP Provisions (BSSC, 2003).

All the amplification factors, F_a (0.1-0.5s) and F_a (0.4-2.0s) are only slightly more than one and they are associated with fairly low levels of earthquake (PGA= 0.06g). In other words, the scaled-to-0.06g earthquake is slightly amplified by the soil in Laho.

4.3.4 Discussion

For the unscaled earthquake with PGA of about 0.0015g, the amplification factors are high, around 2.1 (period 0.4s-2.0s) and 2.2 (period 0.1s-0.5s). However, these amplification factors are associated with very low levels of earthquake shaking which will hardly bring harm to the structure on site.

In contrast, for the scaled earthquake with PGA of about 0.06g, the amplification factors are around 1.05 (period 0.4s-2.0s) and 1.12 (period 0.1s-0.5s). The drastically reduced amplification factors are caused by the nonlinear behaviour of soils which has been explained in chapter 4.1.3. On the other hand, the peak spectral acceleration is around 2.2 at period ranging from 4.7s to 5s which are significantly deviated from the fundamental site period of 2.58s. The peak spectral acceleration and its period should be taken into account during the design of structure because they are associated with PGA of 0.06g which is significant enough to damage the platforms on site, especially if the seismic waves are amplified.

4.4 Summary

Time Series: Amplification of PGA

It is observed that all the unscaled earthquakes, Bintulu earthquake (0.0015g) and Sumatra earthquake (0.0011g) amplify the PGA significantly, especially in Sumandak where the PGA of the first layer (soft soil) is amplified for about 2.75 times. It is also observed that the impedance contrast of shear wave velocities at the boundaries of two layers amplifies the seismic waves.

For the scaled earthquakes (0.06g), the amplification of PGA is drastically reduced due to the nonlinear stress-strain response of soil, resulting in reduced effective shear moduli and increased damping. Besides, the scaled earthquakes (0.06g) only amplify the PGA in Laho but not in Sumandak and Kumang. It is assumed to be caused by the distinct characteristics of the input ground motion. The input ground motion of Sumatra earthquake has a much longer zero-crossing period than the Bintulu earthquake.

Response Spectra: Peak Spectral Amplification

For unscaled earthquakes (0.0015g) in Sumandak, the peak spectral amplification occurs at period 1.1s and 2.7s which does not correspond to the calculated fundamental site period of 3.3s. Conversely, the peak spectral amplification in Kumang and Laho occurs at periods correspond to the calculated fundamental site period.

The scaled earthquakes (0.06g) cause the amplification factors to be greatly reduced due to the nonlinearity of soil. Besides, it is observed that the stronger earthquakes cause the peak spectral amplification to be occurred at a longer period as compared to the unscaled earthquake counterparts. In contrast to the observation for unscaled earthquakes, the peak spectral amplification of Sumandak occurs at period correspond to the fundamental site period. At the same time, the peak spectral amplification of Kumang and Laho occurs at period much longer than the calculated fundament site period.

Amplification Factors: F_a (0.4-2.0s) & F_a (0.1-0.5s)

For the unscaled earthquake, the amplification factors are high but they are associated with very low levels of earthquake (0.0015g) shaking which will not harm the structures on site.

For scaled earthquake, the amplification factors are relatively lower but they are associated with fairly low level of earthquake shaking (0.06g). This level of earthquake shaking is significant enough to damage the platforms on site, especially if the seismic waves are amplified and the structure has a natural period close to the amplified periods. Therefore, the design of structures should take into account the amplification factors and their associated period and level earthquake shaking.

5 CONCLUSION AND RECOMMENDATION

5.1 Conclusion

The unscaled earthquakes that were recorded in Malaysia has a very low level of earthquake shaking (PGA= 0.0015g). Although these earthquake gives a high amplification factor, the amplified earthquake shaking hardly bring any damage to the platforms. The time series of the earthquakes are scaled to 0.06g to simulate the shaking caused by an earthquake with a return period of 475 years in Malaysia. The scaled earthquake gives a much lower amplification factor which is caused by the nonlinear behaviour of soils and a peak spectral amplification at a longer period compared to the unscaled weaker earthquake counterparts. However, the lower amplification factor should be taken into account when necessary in the design of structure because they are associated with PGA of 0.06g which is significant enough to damage the platforms on site, especially if the seismic waves are amplified and the structure has a natural period close to the amplified periods. This research also shows that the impedance contrast of shear wave velocities at the boundaries of two layers amplifies the seismic waves. Besides, the soil amplification factors depend on the intensity of shaking.

5.2 Recommendation

The shear wave velocities estimated from the cone penetration test correlation equation should be compared to the site measured data in the future. The difference in the estimated values and measured values can be used to develop a cone penetration test correlation equation specifically for PMO, SKO and SBO Malaysia. Besides, the estimated bedrock depth and properties should be verified with the site measured data in the future.

REFERENCES

Balendra, T., & Li, Z. (2008). Seismic hazard of Singapore and Malaysia. *Electron J Struct Eng (special issue, Earthquake engineering in the low and moderate seismic regions of Southeast Asia and Australia)*, 57-63.

Balendra, T., Tan, T., & Lee, S. (1990). An analytical model for far-field response spectra with soil amplification effects. *Engineering Structures, 12*(4), 263-268.

Booth, E., Pappin, J., Mills, J., Degg, M., & Steedman, R. (1986). The Mexican Earthquake of 19th September, 1985. *A Field Report by EEFITThe Institution of Civil Engineers, London*.

BSSC, B. S. S. C. (2003). *NEHRP recommended provisions for seismic regulations for new buildings and other structures*: FEMA 450, developed by BSSC for FEMA Washington, DC.

D'Appolonia. (2009). Seismic Hazard Study Phase II for Offshore Sabah, Sarawak and West Malaysia: Amplification for Sites Offshore Malaysia Report (Rev. 1 ed.).

DeMets, C., Gordon, R. G., Argus, D., & Stein, S. (1990). Current plate motions. *Geophysical journal international, 101*(2), 425-478.

Deng, N., & Ostadan, F. (2000). Theoretical and user's manual for SHAKE2000. *Bechtel National Inc., San Francisco, California, January*.

Hashash, Y., Groholski, D., Phillips, C., Park, D., & Musgrove, M. (2012). DEEPSOIL 5.1. *User Manual and Tutorial*.

Kramer, S. L. (1996). Geotechnical earthquake engineering. in prentice–Hall international series in civil engineering and engineering mechanics: Prentice-Hall, New Jersey.

Lam, N. T. K., & Wilson, J. L. (1999). *Estimation of the Site Natural Period from Borehole Records*.

Mahajan, A. (2009). NEHRP soil classification and estimation of 1-D site effect of Dehradun fan deposits using shear wave velocity. *Engineering Geology, 104*(3), 232-240.

Marto, A., Soon, T. C., Kasim, F., & Suhatril, M. (2013). A correlation of shear wave velocity and standard penetration resistance. *EJGE, 18*, 463-471.

Street, R., Woolery, E. W., Wang, Z., & Harris, J. B. (2001). NEHRP soil classifications for estimating site-dependent seismic coefficients in the Upper Mississippi Embayment. *Engineering Geology, 62*(1), 123-135.

Sun, J., & Pan, T.-C. (1995). Seismic characteristics of Sumatra and its relevance to Peninsular Malaysia and Singapore. *Journal of Southeast Asian Earth Sciences, 12*(1), 105-111.

Tan, C. G., Majid, T. A., Ariffin, K. S., & Bunnori, N. M. (2014). Seismic microzonation for Penang using geospatial contour mapping. *Natural Hazards*, 1-14.

Wair, B. R., DeJong, J. T., & Shantz, T. (2012). PACIFIC EARTHQUAKE ENGINEERING RESEARCH CENTER.

APPENDICES

Appendix A: DEEPSOIL v5.1

Description of DEEPSOIL v5.1

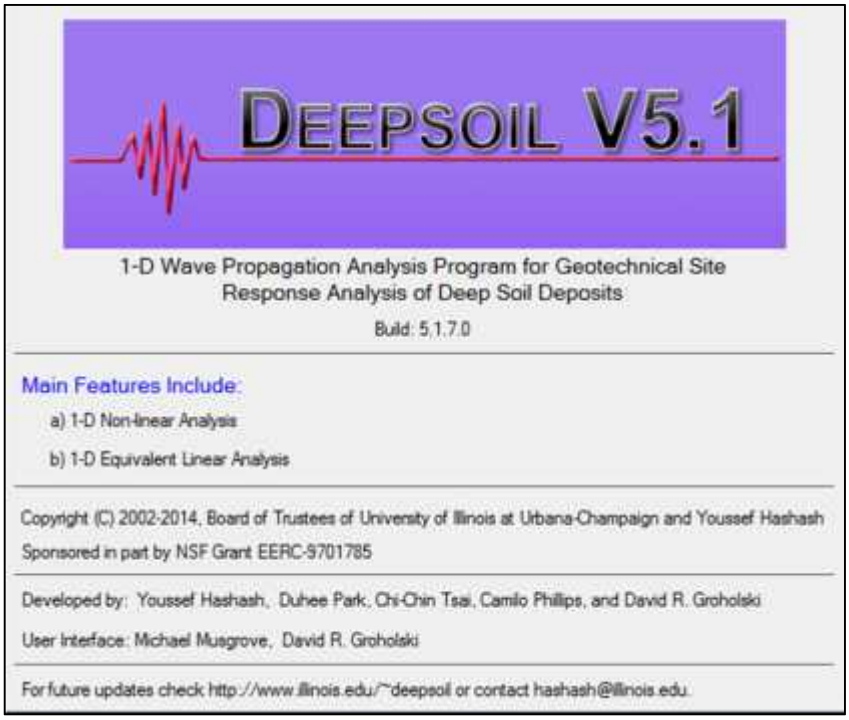

Figure 31 DEEPSOIL v5.1 program description

Screen Shots of DEEPSOIL v5.1 Interface

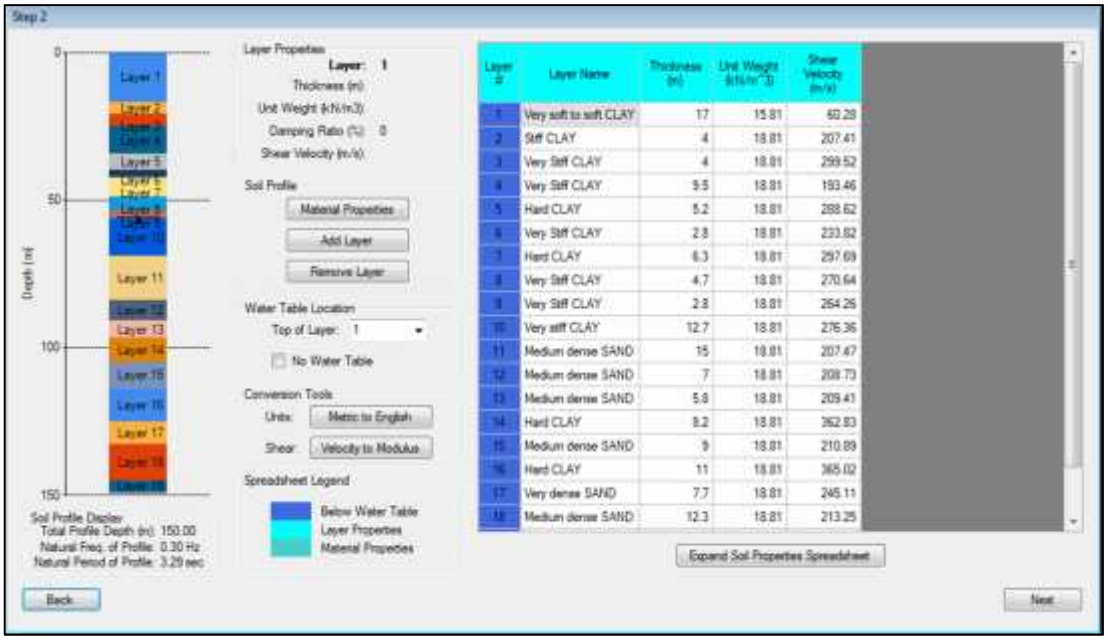

Figure 32 Screen shot of step 2 in DEEPSOIL v5.1 program

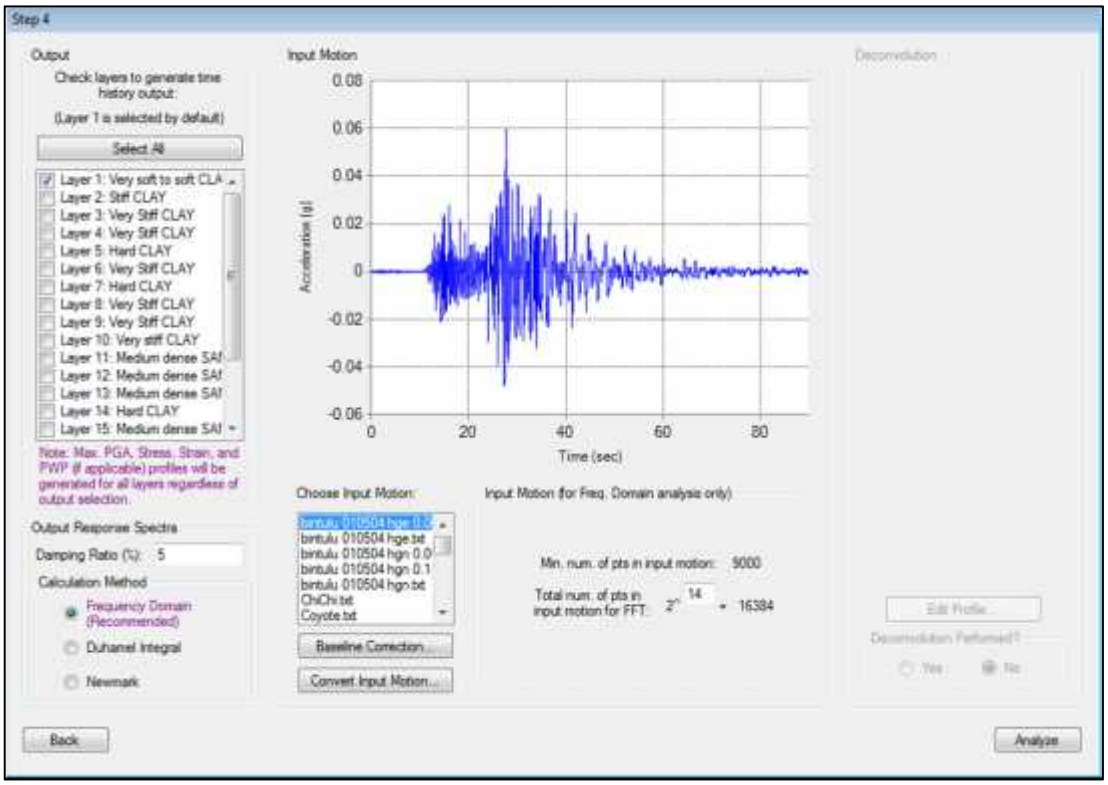

Figure 33 Screen shot of step 4 in DEEPSOIL v5.1 program

Appendix B: Detailed Soil Profile and Soil Properties of the three selected sites

Sumandak

											ALL		SAND		CLAY					
											Eq. 5.6	Eq. 5.7	Eq. 5.11	Eq. 5.13	Eq. 5.16	Eq. 5.17	Eq. 5.18	Eq. 5.19	Eq. 5.20	
Layer	Layer Name	*from* __ *to* __		Thickness (m)	Unit Weight (kN/m^3)	Plasticity Index (%)	Sleeve Friction f_s (kPa)	Corrected Cone Resistance q_t (kPa)	Effective Vertical Stress s'_v (kPa)	Void Ratio, e	Shear Velocity (m/s)		Shear Velocity (m/s)		Shear Velocity (m/s)					**Average Shear Velocity (m/s)**
1	Very soft to soft CLAY	0	17	17	15.81	36	12.5	140	51.00	1.50					68.76	51.06	65.29	38.78	77.51	**60.28**
2	Stiff CLAY	17	21	4	18.81	26	63.65	860	120.00	0.32					275.68	144.07	329.46	121.05	166.78	**207.41**
3	Very Stiff CLAY	21	25	4	18.81	30	93.7	1530	156.00	0.22					402.66	199.58	513.64	173.72	208.03	**299.52**
4	Very Stiff CLAY	25	34.5	9.5	18.81	34	85.55	990	216.75	0.54					225.29	156.80	263.69	132.22	189.32	**193.46**
5	Hard CLAY	34.5	39.7	5.2	18.81	29	129.15	1800	282.90	0.33					350.32	219.96	441.41	192.35	239.07	**288.62**
6	Very Stiff CLAY	39.7	42.5	2.8	18.81	28	121.6	1440	318.90	0.52					263.18	194.31	317.77	167.24	226.61	**233.82**
7	Hard CLAY	42.5	48.8	6.3	18.81	27	158.55	2210	359.85	0.43					334.84	247.46	422.23	218.76	265.19	**297.69**
8	Very Stiff CLAY	48.8	53.5	4.7	18.81	26	143.9	1620	409.35	0.37					321.13	208.16	398.95	180.05	244.91	**270.64**
9	Very Stiff CLAY	53.5	56.3	2.8	18.81	25	149.1	1620	443.10	0.41					306.40	208.35	378.43	180.05	248.07	**264.26**
10	Very stiff CLAY	56.3	69	12.7	18.81	22	159.1	1620	512.85	0.35					329.02	208.69	409.99	180.05	254.04	**276.36**
11	Medium dense SAND	69	84	15	18.81		67	2900	637.50	0.35	251.74	235.44	149.18	193.51						**207.47**
12	Medium dense SAND	84	91	7	18.81		67	2900	736.50	0.33	251.74	235.44	149.18	198.57						**208.73**
13	Medium dense SAND	91	96.8	5.8	18.81		67	2900	794.10	0.32	251.74	235.44	149.18	201.27						**209.41**
14	Hard CLAY	96.8	105	8.2	18.81	24	254.3	2570	857.10	0.32					408.41	272.03	530.41	240.47	Assume	**362.83**
15	Medium dense SAND	105	114	9	18.81		67	2900	934.50	0.30	251.74	235.44	149.18	207.22					soils	**210.89**
16	Hard CLAY	114	125	11	18.81	26	283.95	2700	1024.50	0.33					405.21	280.27	526.55	248.03	below	**365.02**
17	Very dense SAND	125	132.7	7.7	18.81		95.7	9600	1108.65	0.30	273.72	253.83	184.02	268.86					69m are	**245.11**
18	Medium dense SAND	132.7	145	12.3	18.81		67	2900	1198.65	0.33	251.74	235.44	149.18	216.66					Pleistoce	**213.25**
19	Hard CLAY	145	149	4	18.81	28	340.2	3150	1272.00	0.35					417.73	306.40	547.52	273.20	ne	**386.21**
20	Dense SAND	149	150	1	18.81		81.3	4800	1294.50	0.23	266.39	245.42	159.06	241.98						**228.21**

Figure 34 Detailed soil profile and soil properties of site Sumandak

Kumang

Layer	Layer Name	*from __ to __*		Thickness (m)	Submerged Unit Weight (kN/m^3)	Sleeve Friction f_s (kPa)	Shear Velocity (m/s) Vs = 118.8 log(fs) + 18.5
1	Very Soft CLAY	0	1	1	17.81	1.5	39.42
2	Loose SAND	1	3.5	2.5	17.81	4	90.02
3	Firm CLAY	3.5	5.3	1.8	17.81	15.5	159.91
4	Loose to Medium Dense SAND	5.3	7.2	1.9	17.81	12	146.71
5	Stiff CLAY	7.2	10.8	3.6	17.81	32.5	198.11
6	Firm to Stiff CLAY	10.8	31.9	21.1	17.81	51	221.36
7	Medium Dense SAND	31.9	34	2.1	17.81	67	235.44
8	Stiff to Very Stiff CLAY	34	44.9	10.9	17.81	91	251.23
9	Very Stiff CLAY	44.9	51.2	6.3	17.81	109.5	260.78
10	Loose to Medium Dense SILT	51.2	55.8	4.6	17.81	56	226.18
11	Very Stiff CLAY	55.8	60.1	4.3	17.81	120.5	265.72
12	Medium Dense SILT	60.1	68	7.9	17.81	67	235.44
13	Very Stiff CLAY	68	93.8	25.8	17.81	150	277.02
14	Dense SAND	93.8	101.2	7.4	17.81	81	245.23
15	Hard SILT	101.2	109.9	8.7	17.81	200	291.86
16	Hard CLAY	109.9	122	12.1	17.81	200	291.86
17	Dense SAND	122	126	4	17.81	81	245.23
18	Hard CLAY	126	141.4	15.4	17.81	226	298.17
19	Hard CLAY	141.4	146.1	4.7	17.81	250	303.38
20	Dense SAND	146.1	152	5.9	17.81	81	245.23
21	Hard CLAY	152	154.5	2.5	17.81	308.5	314.22
22	Dense SAND	154.5	176	21.5	17.81	81	245.23
23	Hard SILT	176	180	4	17.81	350	320.74

Figure 35 Detailed soil profile and soil properties of site Kumang

Laho

Depth (m)	Description	Submerged Density kN/m^3	Plasticity Index %	Corrected q_t (kPa)	Sleeve Friction f_s (kPa)	Dynamic Pore u_2 (kpa)	Cone Resistance q_c (kPa)	Friction Ratio R_f (%)	Eq. 5.7 for clay V_s	Average V_s	Layer
0	Very stiff CLAY	15.81	30								
5		18.61	35								
10	Stiff CLAY	18.31	47								
15	Very Stiff CLAY	18.31	28	2,000	20	1,000	1,750	1	173.06		
20	Stiff to very stiff CLAY	18.61	21	2,000	20	1,250	1,688	1	173.06	173.06	1
25		18.31		2,000	20	1,250	1,688	1	173.06		
30		18.61		2,000	30	1,250	1,688	1.5	193.98		
35		18.11		2,500	30	1,500	2,125	1.5	193.98	193.98	2
40		17.61	43	2,500	30	1,500	2,125	1.5	193.98		
45		18.41		2,500	40	1,500	2,125	1.5	208.82		
50		18.71		2,500	40	1,500	2,125	1.5	208.82	208.82	3
55		18.61		3,000	40	2,000	2,500	1.5	208.82		
60		18.31	38	3,000	40	2,000	2,500	1.5	208.82		
65		18.61		3,000	50	2,000	2,500	1.5	220.34		
70	Stiff to very stiff CLAY	17.81	54	4,000	60	2,000	3,500	1.5	229.74	225.04	4
75		18.51		4,000	60	2,000	3,500	1.5	229.74		
80		18.21		4,000	50	2,000	3,500	1.5	220.34		
85	Very stiff to hard CLAY	18.11		4,000	65	2,000	3,500	1.5	233.87	231.81	5
90		18.61		4,000	60	2,000	3,500	1	229.74		
95		18.61	26	4,000	50	2,000	3,500	1	220.34	220.34	6
100		18.01		4,000	50	2,000	3,500	1	220.34		
105	Medium dense to dense SAND	18.71		12,500	80	300	12,425	0.5	244.59	198.71	7
110		18.81		17,500	120	300	17,425	0.5	265.51	265.51	8
115		18.91		17,500	120	300	17,425	1	265.51		
120		18.81		20,000	120	300	19,925	0.5	265.51	265.51	9
125		18.81		20,000	120	300	19,925	0.5	265.51		
130	Very stiff to hard CLAY	18.01	24	5,500	50	3,000	4,750	0.5	220.34	220.34	10
135		18.71	23	5,500	50	3,000	4,750	0.5	220.34		
140		18.01		5,500	70	3,000	4,750	0.5	237.70		
145		18.01		6,000	80	2,000	5,500	1	244.59	242.29	11
150		18.01		6,000	80	2,000	5,500	1	244.59		

Figure 36 Detailed soil profile and soil properties of site Laho